Genome-wide meta-analysis of pneumonia suggests a role for mucin biology and provides novel drug repurposing opportunities

William R. Reay[1,2], Michael P. Geaghan[1,2], 23andMe Research Team[3†], Murray J. Cairns[1,2*]

[1]School of Biomedical Sciences and Pharmacy, Faculty of Health and Medicine, The University of Newcastle, Callaghan, NSW, 2308, Australia

[2]Hunter Medical Research Institute, Newcastle, NSW, 2305, Australia

[3]23andMe Inc., Sunnyvale, CA, 94086, United States of America

[†]A list of authors and their affiliations appears at the end of the paper

[*]To whom correspondence should be addressed:
Professor Murray Cairns, Medical Sciences Building, University Drive, Callaghan, NSW 2308, Australia
Email: Murray.cairns@newcastle.edu.au, Phone: +61 02 4921 8670

ABSTRACT

Pneumonia remains one of the leading causes of death worldwide, particularly amongst the elderly and young children. We performed a genome-wide meta-analysis of lifetime pneumonia diagnosis (N=266,277), that encompassed the largest collection of cases published to date. Genome-wide significant associations with pneumonia were uncovered for the first time beyond the major histocompatibility complex region, with three novel loci, including a signal fine-mapped to a cluster of mucin genes. Moreover, we demonstrated evidence of a polygenic effect of common and low frequency pneumonia associated variation impacting several other mucin genes and *O*-glycosylation, further suggesting a role for these processes in pneumonia pathophysiology. The pneumonia GWAS was then leveraged to identify drug repurposing opportunities, including evidence that supports the use of lipid modifying agents in the prevention and treatment of the disorder. We also propose how polygenic risk could be utilised for precision drug repurposing through pneumonia risk scores constructed using variants mapped to pathways with known drug targets. In summary, we provide novel insights into the genetic architecture of pneumonia susceptibility, with future study warranted to functionally interrogate novel association signals and evaluate the suitability of the compounds prioritised by this study as repositioning candidates.

INTRODUCTION

Pneumonia is characterised as an acute infection of the lung, with fluid filled alveoli and resultant restriction of oxygen intake being a key hallmark of its pathophysiology. There are a number of mechanisms known to cause pneumonia, however, bacterial or viral infection are the most common aetiologies[1]. Pharmacological intervention in pneumonia treatment is largely dependent on the infection source – for instance, bacterial induced pneumonia is treated with antibiotics. Yearly mortality rates worldwide from pneumonia remain high, even in the developed world where access to antibiotics and routine hospital care is usually unrestricted[2,3]. This necessitates a greater understanding of the mechanisms involved in pneumonia susceptibility and pathogenesis, which could be leveraged to identify novel treatments and inform the repositioning of existing drugs.

There has been considerable work undertaken to identify host factors which influence the onset and clinical course of pneumonia. Twin-based estimates of pneumonia heritability are still lacking, however, the heritability of death due to infections disease has been estimated as high as 40%, although further study is required [4]. There have also been few studies which have used modern statistical genetics approaches to test for the existence of risk-increasing or protective alleles associated with pneumonia with sufficient power for surpassing genome-wide significance. Previously, a genome-wide association study of lifetime self-reported pneumonia diagnosis was published using participants obtained by 23andMe Inc. that identified a significant signal in the major histocompatibility complex (MHC) region on chromosome six[5]. We sought to increase statistical power to detect association signals by performing a genome-wide meta-analysis of self-reported pneumonia in the 23andMe cohort with SNP effects on a clinically ascertained pneumonia phenotype from the FinnGen consortium. The genetic architecture of pneumonia was further interrogated to identify novel risk genes and salient biological pathways, along with an estimate of genetic correlation with clinically significant phenotypes. These data were then considered in light of drug repurposing and provided support to a number of plausible repositioning opportunities.

MATERIALS AND METHODS

Genome-wide meta-analysis of pneumonia

The genome-wide meta-analysis was performed using two primary study cohorts from 23andMe Inc. and FinnGen (release 3), respectively, with full details of these cohorts and the meta-analysis procedure detailed in the supplementary methods. Summary statistics for a self-reported pneumonia phenotype were obtained from 23andMe as outlined by Tian *et al.*[5]. This self-reported phenotype was derived from an online survey of 23andMe customers about their medical history. In the final GWAS after quality control (QC), there were 40600 cases and 90039 controls. In addition, summary statistics for pneumonia were downloaded from the third release of the FinnGen database which combines genotype data from Finnish biobanks and digital health record data from Finnish health registries. The pneumonia phenotype chosen was *All pneumoniae* (J10 pneumonia), for which 15771 cases and 119867 controls were available for GWAS after QC.

The 23andMe and FinnGen summary statistics were meta-analysed using an inverse-variance weighted model with fixed effects as implemented by METAL version March 2011[6]. Firstly, we meta-analysed common variants, defined as sites with allele frequency > 1% in both the 23andMe and FinnGen cohorts. Variants were retained if they were available in both summary statistics and had an imputation quality that exceeded a minimum of 0.3 or a mean of 0.5 for variants not physically genotyped, resulting in 6888413 sites with an effect size estimate from the meta-analysis and a total sample size of 266277 individuals. Imputed rare variants available in both studies were subjected to a stricter filtering threshold for imputation quality such that only variants with a minimum imputation quality > 0.5 or a mean value > 0.7 were subjected to meta-analysis, with 834366 low frequency variants considered. In both instances, we further tested for heterogeneity between the contributing studies using Cochran's *Q* test. Genome-wide summary statistics from the IVW meta-analysis were processed using the FUMA v1.3.6 (Functional Mapping and Annotation of Genome-Wide Association Studies) platform[7]. Genome-wide significant variants were characterised using the traditional $P < 5 \times 10^{-8}$ threshold, whilst suggestive significance was defined using a more lenient threshold of $P < 1\times10^{-5}$. We utilised the default settings for defining independent significant SNPs ($r^2 \leq 0.6$) and lead SNPs ($r^2 \leq 0.1$). The reference panel population for LD estimation was the UK biobank release 2b 10k White British panel, with LD blocks within 250 kb of each other merged into a single locus. We examined the effect of conditioning on two smoking GWAS via the

103 multi-trait-based conditional & joint analysis (mtCOJO) framework implemented in GCTA v
104 1.93.2 beta (Supplementary Methods)[8,9]. For the *MUC5AC* lead SNP, we additionally
105 performed a phenome-wide association study using the IEUGWAS database version 3.7.0
106 (https://gwas.mrcieu.ac.uk/), reporting SNPs using a conventional phenome-wide significance
107 threshold of $P < 1 \times 10^{-5}$. Given the most significant association in this database was a GWAS
108 of adult-onset asthma [10], we tested whether the association of SNPs proximal to *MUC5AC* was
109 driven by the same underlying causal variant, assuming a single causal variant, via the *coloc*
110 colocalisation methodology implemented in version 4 of the package [11]. We also sought to
111 replicate our results in two UK biobank (UKBB) pneumonia GWAS, specifically, a self-
112 reported pneumonia phenotype performed in the automated GWAS pipeline by the MRC IEU
113 group (ukb-b-4533, https://gwas.mrcieu.ac.uk/datasets/ukb-b-4533/), as well as a phecode
114 ICD-10 UKBB GWAS performed in an automated series of GWAS by the authors of the
115 SAIGE methodology (https://pheweb.org/UKB-SAIGE/pheno/480) [12].
116
117 **Estimation of SNP-based heritability**
118 SNP based heritability was computed using LD score regression (LDSR) with 1000 genomes
119 phase 3 LD scores and weights[13]. We converted the heritability estimate to the liability scale
120 assuming the population prevalence of pneumonia as that of pneumonia in the FinnGen dataset
121 (12.61%), as well as a more conservative estimate based on ICD-10 diagnosed pneumonia in
122 the UK biobank (UKBB) sample (3.20% - Supplementary Methods).
123
124 **Finemapping genome-wide significant loci**
125 We finemapped the three-novel genome-wide significant loci outside of the MHC region by
126 using a method which leverages asymptotic Bayes' factors (ABF) to estimate credible sets
127 under the assumption of a single causal variant[14]. Specifically, we utilised Wakefield's method
128 to approximate ABFs assuming a prior variance of 0.2^2, which reflects the belief that the
129 confidence intervals of estimated variant effect sizes expressed as odds ratios ranging from
130 around 0.68 to 1.48. Given that the posterior probability for causality of each variant is
131 proportional to its Bayes' factor, these can be summed until a prespecified probability (ρ) is
132 reached, thus, constituting a ρ set of putative causal variants. In this study, we derived 95%
133 credible sets. A single causal variant was assumed such that we did not have to account for LD
134 between variants, which has been demonstrated to be problematic in finemapping studies
135 which prespecify more than one causal variant using references external to the GWAS like the
136 1000 genomes project panel[15].

137 **Gene-based and gene-set association**

138 Common variant (MAF > 0.01) SNP-wise *P* values were aggregated at gene-level using
139 MAGMA v1.07b[16], as described in the supplementary methods. The Bonferroni threshold for
140 genic association was $P < 2.68 \times 10^{-6}$, accounting for the number of genes tested. Moreover,
141 gene-based *P* values were leveraged for gene-set association using 1379 hallmark and
142 canonical gene-sets from the Molecular Signatures Database (MSigDB)[17]. Rare variants (MAF
143 < 0.01) were also aggregated at gene-level by leveraging the properties of the Cauchy
144 distribution (Supplementary Methods). Code for the Cauchy combination test was obtained
145 from (https://github.com/yaowuliu/ACAT) and outlined by Liu and Xie[18,19]. The MAGMA
146 approach for common variants accounts for dependency between *P* values by estimating their
147 covariance as a function of pairwise LD in a population sample – however, there are
148 methodological challenges with this approach for rare variants and likely much larger samples
149 would be required for accurate estimation of dependency between rare variants, if any
150 exists[20,21]. Therefore, we employed Cauchy transformation to combine *P* values as it guards
151 against type I error inflation due to potential unknown covariance between rare variants
152 (Supplementary Methods). In addition, we constructed a model for rare variant gene-set
153 association analogous to the MAGMA approach for common variants that leverages gene-
154 based *Z* values (probit transformation of *P*). The same collection of pathways from MSigDB
155 were considered, with genic *Z* values regressed against a binary indicator of set membership
156 (β_S), covaried for logarithmically transformed gene-length, and rare variant count per gene. A
157 one-sided test was performed for β_S, such that the null hypothesis is $\beta_S = 0$ and the alternative
158 $\beta_S > 0$. Only gene-sets with rare variants overlapping at least 5 genes were retained.

159

160 **Transcriptome-wide association studies of pneumonia**

161 A transcriptome-wide association study (TWAS) of pneumonia was performed using the
162 FUSION package[22]. We utilised GTEx v7 SNP weights from three tissues that would be
163 plausibly involved in the pathophysiology of pneumonia (whole blood, lung, and spleen). We
164 corrected for the number of *cis*-heritable genes outside the MHC region for which a TWAS *Z*
165 could be calculated in each tissue (Supplementary Methods). For transcriptome-wide
166 significant genes, we tested whether the expression and pneumonia-associated signal displayed
167 statistical colocalisation as encompassed by the SNP weights with the *coloc* package as
168 implemented by FUSION[11]. In addition, we probabilistically finemapped transcriptome-wide
169 significant regions using the FOCUS approach to derive a credible set of putative causal genes,
170 as described previously[23]. We utilised the default Bernoulli prior ($p = 1 \times 10^{-3}$) and chi-square

171 prior variance ($n\sigma^2$ = 40) to approximate Bayes' factors for each gene, and thus, derive the
172 posterior inclusion probabilities (*PIP*) for each gene to be causal given its observed TWAS *Z*.
173
174
175 **Genetic correlation and causal inference**
176 We estimated genetic correlation between pneumonia and 180 high quality, European ancestry
177 GWAS using LDSR as implemented by the LDhub application[24]. For Bonferroni significant
178 genetic correlation estimates, we constructed a latent causal variable (LCV) model using the
179 most significant trait from each LDhub phenotypic category and pneumonia to evaluate
180 evidence for genetic causality between traits, as outlined extensively elsewhere[25–27]. A strong
181 estimate of the posterior genetic causality proportion (GCP) was defined as significantly
182 different from zero (one sided *t*-test) and an absolute GCP estimate > 0.6. Weak GCP estimates
183 close to zero for genetically correlated traits imply that their relationship is potentially mediated
184 by horizontal pleiotropy, whereby there are shared pathways, but the two traits do not likely
185 exhibit vertical pleiotropy by acting within the same pathway. We additionally evaluated
186 evidence for a causal relationship between HDL cholesterol and pneumonia by constructing a
187 multivariable Mendelian randomisation (MR) model using the TwoSampleMR package[28]. This
188 multivariable model leveraged genetic instrumental variables (IV) from three highly
189 biologically interconnected lipid traits (LDL, HDL, and triglycerides) and estimated the effects
190 of these IVs on the outcome conditioned on their association with the other two lipid classes[29].
191
192 **Genetically informed drug repurposing**
193 We implemented three strategies to propose drug repurposing candidates: i) single loci drug-
194 gene matching, ii) genetic correlation and/or evidence of a putative causal relationship between
195 a biochemical trait that could be targeted by an approved drug, and iii) precision drug
196 repurposing using the polygenic scoring orientated *pharmagenic enrichment score* (PES)
197 approach. Full details of these analyses are described in the supplementary methods. We
198 utilised a panel of 50 biochemical GWAS performed by the Neale lab from the UK biobank
199 which had high or medium confidence estimates of SNP heritability that were significantly
200 different from zero (http://www.nealelab.is/uk-biobank) and estimated genetic correlation and
201 the posterior mean GCP for trait pairs that survived Bonferroni correction. We sought to
202 replicate the results of the multivariable MR for the three lipid classes (LDL, HDL, and
203 Triglycerides) using the UK biobank GWAS. MR was then performed to evaluate further
204 evidence for a causal effect between gamma-glutamyltransferase (GGT) and pneumonia, as

205 well as triglycerides and pneumonia (univariable estimate). Specifically, we defined
206 independent, non-palindromic genome-wide significant variants as IVs and constructed four
207 MR models with differing underlying assumptions (two inverse-variance weighted estimators
208 with fixed or multiplicative random effects, weighted median estimator, weighted mode
209 estimator, and MR-Egger)[30–33]. A series of sensitivity analyses to evaluate statistical evidence
210 for confounding pleiotropy was then undertaken as outlined in the supplementary methods[32–
211 35].
212
213 The PES framework is based on the postulation that an enrichment of genetic risk within a
214 biological pathway with known drug targets may be an impetus to repurpose a drug which
215 modulates that pathway for individuals who carry the high genetic load mapped to the pathway,
216 as described elsewhere[36,37]. Specifically, we identify druggable pathways with an enrichment
217 of common variant associations relative to the rest of the genes tested and construct pathway-
218 based risk scores for these gene-sets (Supplementary Methods). We utilised the UK biobank
219 (UKBB) cohort to test the association between a pneumonia PES and pneumonia phenotypes
220 recorded for these participants[38,39]. These analyses are described in detail in the supplementary
221 methods. Briefly, we retained 336,896 unrelated white British ancestry participants and
222 13,568,914 autosomal variants that survived a series quality control steps, including,
223 imputation quality filtering (INFO > 0.8), MAF > 1×10^{-4}, call rate > 0.98, and filtering strong
224 deviations from the Hardy-Weinberg equilibrium. Self-reported pneumonia diagnosis and
225 ICD-10 codes from hospital inpatient records were used to construct the pneumonia phenotype
226 (Supplementary Methods). There were 10,540 individuals from the genotyped subset of the
227 cohort included in the PES calculation with a primary or secondary diagnosis using the ICD-
228 10 primary or secondary diagnosis codes relevant to pneumonia. In the strict phenotype
229 definition, we defined cases as those satisfying ICD-10 criteria, and controls as all those who
230 did not have one of those codes recorded along with any individual who self-reported
231 pneumonia without a pneumonia ICD-10 code ($N_{Controls}$ = 320,213). Individuals who self-
232 reported pneumonia but were not assigned a relevant ICD-10 code were excluded from the
233 study cohort in this strict configuration. In the broad-phenotype definition, pneumonia cases
234 were individuals with a relevant ICD-10 code or a self-reported lifetime pneumonia diagnosis
235 (N = 15,138). In other words, the strict definition only included individuals with a pneumonia
236 ICD-10 code. The PES was then constructed using common, autosomal variants outside of the
237 MHC region mapped to genes in that pathway with PRsice2 assuming an additive model, with
238 further details provided in the supplementary methods[40]. The *P* value threshold of including

239 variants in the PES was the same as what was used to identify the gene-set. A genome wide
240 PRS for pneumonia susceptibility was also constructed in an analogous fashion.
241
242 We explored the phenotypic relevance of pneumonia PES profiles using a random subset of
243 the UKBB (N ~ 10,000) for which a multiplex assay was performed to quantity
244 immunoglobulin G (IgG) antibody response to a series of antigens for infectious agents
245 selected for study, as outlined elsewhere[41]. The two phenotypes of interest here were a binary
246 indicator of *seropositivity* for 14 infections with seroprevalence > 5% in our genotyped subset
247 of the cohort, and amongst seropositive individuals, a continuous measure of antibody response
248 (mean fluorescence intensity) to each antigen for that infection – termed *seroreactivity*. The
249 correlation between PES or PRS and seroreactivity was assessed by linear regression, whilst
250 logistic regression was utilised for seropositivity. Both models were covaried for sex, age, age^2,
251 ten SNP derived principal components, genotyping batch, and two QC metrics related to the
252 antibody assay (Supplementary Methods). A heatmap of the regression *t* statistics was
253 constructed using the ComplexHeatmap package[42]
254
255 **RESULTS**
256
257 **Novel common and rare variant loci associated with pneumonia**
258 We performed a genome-wide meta-analysis of pneumonia using common and rare (MAF <
259 0.01) overlapping variants from 23andMe and FinnGen release three, with 6,888,413 and
260 834,366 common and low frequency sites tested, respectively. We estimated the SNP based
261 heritability as approximately 3.24% on the liability scale (Fig. 1b), using the incidence of
262 pneumonia in the FinnGen cohorts as the population prevalence (12.67%), although we
263 acknowledge the population prevalence of pneumonia is difficult to quantify. As a result, we
264 re-estimated h^2 using a more conservative population prevalence value based on phenotype
265 data from the UK biobank (3.20%), resulting in a lower estimate of $h^2_{SNP} = 0.0213$. The point
266 estimate of SNP-based h^2 was higher in the 23andMe cohort. $h^2_{SNP} = 0.054$, although the
267 estimate was more precise in the meta-analysis than in 23andMe and FinnGen alone: Z_{Meta} =
268 9.26, $Z_{23andMe} = 7.44$, and $Z_{FinnGen} = 4.12$. In line with previous comparisons between self-
269 reported and clinically ascertained phenotypes, the heritability estimate was lower in FinnGen
270 than 23andMe. There was some evidence of test statistic inflation when visualised as a *QQ* plot
271 (Supplementary Figure 1), however, the proportion of the polygenic signal in the meta-analysis

272 attributed to model misspecification and/or confounding was around 11% (LDSR ratio =
273 0.1145), whilst the mean χ^2 was large enough to estimate heritability (1.11).
274
275 There were four common genomic loci that surpassed the conventional genome-wide
276 significance threshold ($P < 5 \times 10^{-8}$, Table 1, Fig. 1a,c, Supplementary Fig. 2-5). The effect
277 sizes of these common variant signals were small in accordance with expectation, with each
278 SNP increasing or decreasing the odds of pneumonia by around 5%. Unsurprisingly, the most
279 significant signal spanned the major histocompatibility complex (MHC) region, which has
280 been previously published as associated with pneumonia in the 23andMe cohort[5]. Due to the
281 complexity of this region, we define the MHC signal as a single locus, with the minor allele of
282 the lead common SNP associated with a small reduction in the odds of pneumonia (OR = 0.94
283 [95% CI: 0.92, 0.96], $P = 6.44 \times 10^{-13}$). The most significant novel common signal in this study
284 was a region located on chromosome 11, with the lead SNP (rs28624253) located upstream of
285 the *MUC5AC* gene that encodes a mucin protein, with three other genes that encode a mucin
286 protein within 400 kilobases of the lead SNP *MUC6*, *MUC2*, and *MUC5B*. Importantly,
287 rs28624253 was similarly associated in the 23andMe ($P = 2.65 \times 10^{-6}$) and FinnGen ($P = 3.42$
288 $\times 10^{-6}$) cohorts and there was no appreciable evidence for differences in population structure
289 between the input GWAS driving this signal. Mucins are heavily glycosylated proteins that
290 play a number of important roles, particularly in relation to the maintenance of mucosal
291 barriers[43] . Mucin genes are known the exhibit somewhat pervasive genomic complexity and
292 evidence of heterogeneity between populations, to ensure that this signal is not just an artefact
293 of this, we performed a phenome-wide association study of the lead SNP and found that this
294 variant was associated with only relevant phenotypes to pneumonia. Specifically, it was linked
295 to adult-onset asthma, self-reported regular cough and mucus, and eosinophil count at a
296 conventional phenome-wide significance threshold ($P < 1 \times 10^{-5}$). Given rs28624253 was
297 associated with adult-onset asthma at a more stringent level of genome-wide significance, we
298 tested whether the mucin signal observed for pneumonia and adult-onset asthma were driven
299 by the same underlying causal variant and found strong evidence to support this hypothesis
300 (posterior probability > 90%). We caution that this assumes the existence of a single causal
301 variant, which may be unrealistic given the complexity of this region. As we visualise in
302 supplementary figure 6, if one utilises a more conservative prior probability of a shared causal
303 variant than there is some evidence that there is a different underlying causal variant but that
304 the locus is still associated with both traits. It should also be noted that the odds increasing
305 allele for pneumonia (*G*) is perhaps counterintuitively associated with decreased risk of asthma,

306 which suggests a multifaceted biological mechanism which may be related to the role of mucins
307 in the airway.
308
309 The third most significant locus encompassed several genes including *SAMD8*, *DUSP13*, and
310 *VDAC2*, whilst locus four was largely intergenic, with some variants overlapping long-
311 noncoding RNAs with limited annotation information (Supplementary Text). There were also
312 two loci that almost surpassed genome-wide significance; specifically, a locus physically
313 mapped to the interleukin-6 receptor region (*IL6R* – lead SNP: rs12730036, $P = 5.61 \times 10^{-8}$),
314 and a region on chromosome 12 where the lead SNP is mapped to an intron of *TNFRSF1A*,
315 which encodes a tumour necrosis factor receptor (lead SNP: rs1800693, $P = 5.5 \times 10^{-8}$). We
316 integrated functional genomic and annotation data to prioritise candidate genes from the novel
317 genome-wide significant loci in this study, as described in the supplementary text. We found
318 that genes in the non-MHC loci implicated by at least two lines of evidence were enriched in
319 phenotypically relevant pathways such as mucus layer, lung fibrosis, and *O*-linked
320 glycosylation of mucins (Supplementary Figure 5, Supplementary Text). .Interestingly, despite
321 the meta-analysis combining a self-reported phenotype with clinically ascertained pneumonia
322 diagnoses, only the lead SNP in the MHC locus demonstrated any significant heterogeneity in
323 the effect sizes between the two cohorts (Cochran's Q, $P_{\text{Het}} = 0.04$, Table 1, Supplementary
324 Text, Supplementary Figure 7).
325
326
327
328
329
330
331
332
333
334
335
336
337
338
339

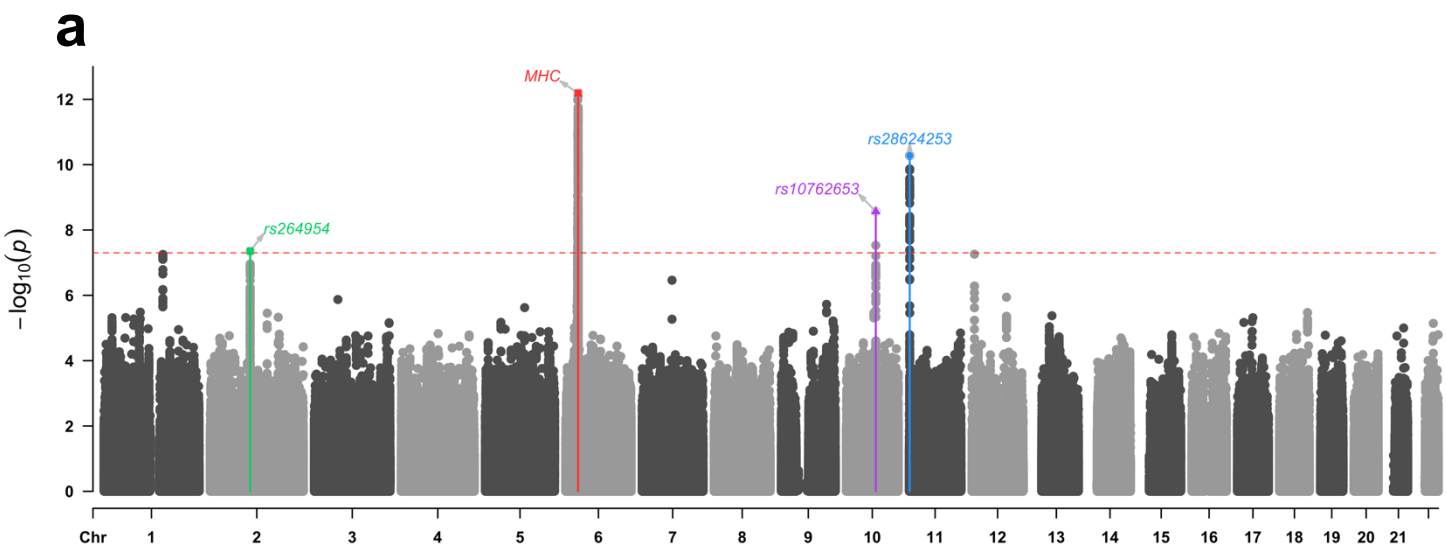
a
MHC
rs28624253
rs10762653
rs264954
−log10(p)
Chr

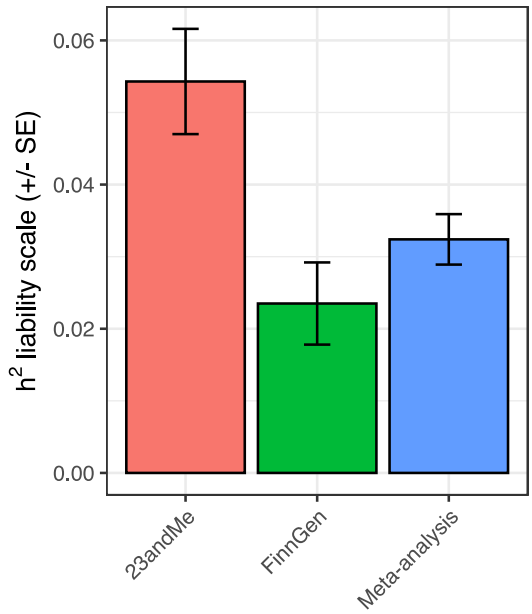
b
h2 liability scale (+/- SE)
23andMe
FinnGen
Meta-analysis

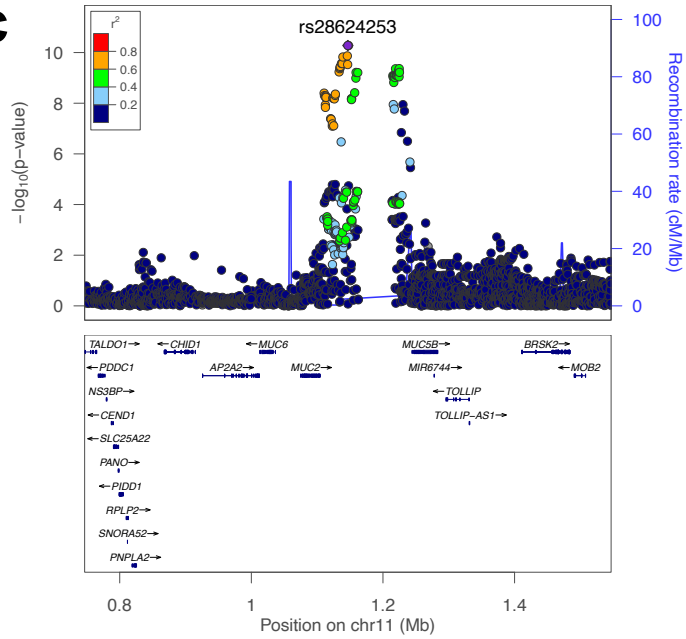
c
rs28624253
−log10(p−value)
Recombination rate (cM/Mb)
Position on chr11 (Mb)

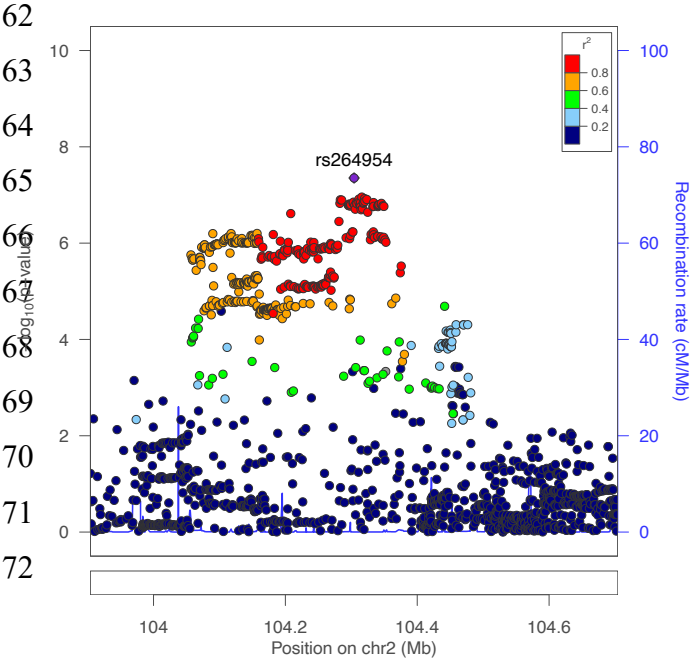
rs264954
−log10(p−value)
Recombination rate (cM/Mb)
Position on chr2 (Mb)

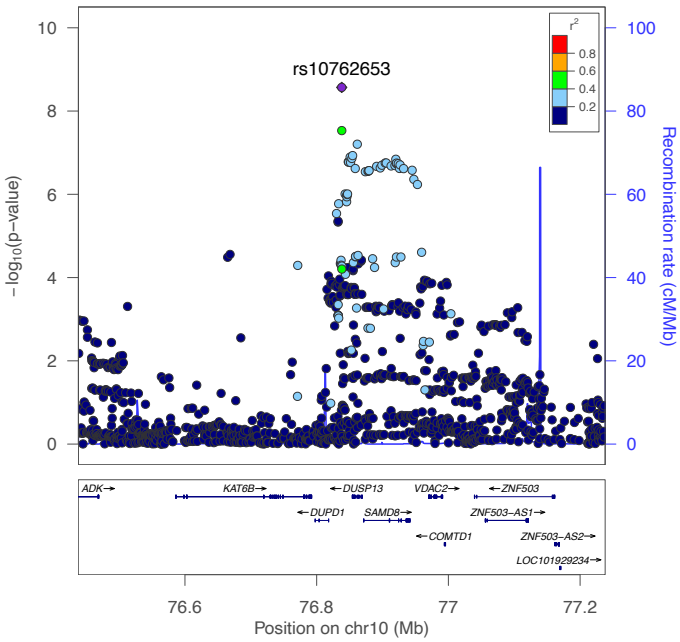
rs10762653
−log10(p−value)
Recombination rate (cM/Mb)
Position on chr10 (Mb)

373 **Figure 1. Genome-wide meta-analysis of pneumonia susceptibility.** (**a**) Manhattan
374 plot of common variant GWAS for pneumonia, as is usual practice, each point is the -
375 $\log_{10}$ *P* value of a variant for association with pneumonia, with the red dotted line
376 indicative of genome-wide significance ($P < 5 \times 10^{-8}$). Lead SNPs are highlighted and
377 labelled on the plot, except for the MHC locus which we denote as "MHC" due to its
378 complexity. (**b**) Estimates of SNP-based heritability (h^2) on the liability scale for the
379 23andMe and FinnGen cohorts individually, as well as the using the inverse-variance
380 weighted effects meta-analysis of the two cohorts. The error bars represent the standard
381 error of h^2. (**c**) Region plots for the three-novel genome-wide significant loci outside of
382 the MHC region, the LD for each variant with the lead SNP estimates from the 1000
383 genomes phase III European reference set was utilised to colour the points.
384
385 **Table one: Lead SNPs within common genome-wide significant loci associated with**
386 **pneumonia**

Lead SNP	Locus	EA/NEA	EAF (NFE)	EAF (FIN)	OR	95% CI	P_{GWAS}	P_{Het}
rs9268966	MHC	G/A	0.26	0.33	0.94	0.92, 0.96	$6.44e^{-13}$	0.04
rs28624253	chr11:1110395-1232702	G/A	0.37	0.41	1.05	1.04, 1.07	$5.27e^{-11}$	0.44
rs10762653	chr10:76815686-76993015	G/A	0.16	0.18	1.06	1.04, 1.08	$2.70e^{-9}$	0.61
rs264954	chr2:104056454-104380545	T/C	0.46	0.45	0.96	0.95, 0.98	$4.44e^{-8}$	0.53

387 Common (MAF > 0.01) lead SNPs were defined as independent SNPs ($r^2 < 0.1$) within each genomic locus.
388 The effect allele (EA) and non-effect allele (NEA) was reported for this table such that the effect allele was the
389 minor allele. The effect allele frequency (EAF) is denoted in gnomAD v2.1.1 for non-Finish Europeans (NFE)
390 and Finns (FIN). All odds ratio and their respective confidence intervals were calculated relative to the EA.
391 Heterogeneity of effect between the 23andMe and FinnGen cohorts was tested using Cochran's *Q*, with the *P*
392 value of that test reported here (P_{Het}). Due to the complexity of locus 1 (MHC), we report only a single common
393 SNP for this locus. Locus coordinates in in hg19 assembly.
394
395 The novel genome-wide significant loci outside the MHC region were finemapped to estimate
396 a 95% credible set of plausible causal variants assuming a single causal variant in each region
397 (Supplementary Tables 1-3). The variants encompassed by the 95% credible set for the

398 rs28624253 locus were all proximally upstream/downstream of *MUC5AC*, or within the gene
399 itself, supporting the relevance of this mucin gene for that association signal. The second most
400 significant novel pneumonia associated locus discovered in this study (rs10762653 lead SNP)
401 had a smaller credible set, with the lead SNP having a considerably high posterior probability
402 than the remaining credible set SNPs (*PP* = 0.676). Interestingly, the lead SNP for this locus
403 has low estimated LD with other proximal genome-wide significant SNPs (Fig 1c), suggesting
404 the existence of several causal variants that cannot be accounted for by this method. Finally,
405 the intergenic region spanned by the third novel genome-wide significant locus yielded a large
406 credible set of over 200 variants and, as a result, further functional interrogation is required to
407 mechanistically interpret this locus.
408
409 Smoking status was not included as a covariate in the respective GWAS meta-analysed, and
410 thus, we sought to investigate whether genetic variants associated with smoking may confound
411 our findings in this GWAS. Specifically, we genetically conditioned common variant
412 associations on their effect size from a GWAS of smoking initiation and smoking heaviness
413 using mtCOJO[8]. The effect sizes of the lead SNPs from the novel genome-wide significant loci
414 were not greatly attenuated after conditioning on either of the smoking phenotypes and
415 remained genome wide significant, with the exception of the locus tagged by rs264954
416 (Conditioned on smoking initiation: $P = 7.15 \times 10^{-7}$; Conditioned on smoking heaviness: $P =$
417 1.05×10^{-7}). Furthermore, there was a slight reduction in the SNP heritability estimate on the
418 liability scale, although this only amounted to a less than 0.5% difference after conditioning on
419 either smoking phenotype – $h^2_{\text{Conditioned on smoking initiation}} = 3.08\%$, $h^2_{\text{Conditioned on smoking heaviness}} =$
420 2.95%.
421
422 We also uncovered a genome-wide significant association between a rare intergenic variant in
423 the MHC region and pneumonia - rs11962863, OR = 1.59 [95% CI: 1.44, 1.74], $P = 1.15 \times 10^{-}$
424 ^{9}. This relatively large effect allele, however, did display statistically significant heterogeneity
425 in its effect between the two cohorts ($P = 8.20 \times 10^{-5}$). This locus is considerably rarer in the
426 Finnish population (AF = 5.8×10^{-4}) than non-Finnish Europeans in gnomAD (AF = $2.9 \times 10^{-}$
427 ^{3}), which may account for its larger effect size in the FinnGen cohort. Due to the complexity
428 of recombination and linkage in the MHC locus, the functional consequences of this variant
429 remains difficult to interpret at an individual level without considering the local genomic
430 context of affected individuals, such as HLA type. We also detected six additional regions with

431 rare variants that surpassed suggestive significance for association with pneumonia ($P < 1 \times$
432 10^{-5}, Supplementary Table 4).
433
434 We sought to replicate our genome-wide significant and suggestively associated common loci
435 using two GWAS from the independent UK Biobank cohort – specifically, we utilised two
436 automated GWAS that encompassed a self-reported pneumonia phenotype (N_{Case} = 6572,
437 $N_{Controls}$ = 456,361) and ICD-10 derived pneumonia diagnoses (N_{Case} = 10,059, $N_{Controls}$ =
438 398,538). We investigated both phenotyping approaches given our GWAS was a meta-analysis
439 of self-reported and clinically ascertained data. In the self-reported pneumonia UKBB GWAS,
440 we found that no SNPs replicated at genome-wide significance, however, the *MUC5AC* lead
441 SNP was nominally associated in the same direction (β = 0.001, SE = 2.6 x 10^{-3}, P = 0.022),
442 with the MHC lead SNP also was also nominally significant (P = 0.03) and the remaining two
443 lead SNPs demonstrated no significant evidence of replication. The ICD-10 phenotype GWAS
444 in the UKBB did not replicate any of our non-MHC genome-wide significant SNPs at even
445 nominal significance, although MHC SNPs were found to be nominally significant. It should
446 be noted that a limitation of both GWAS is that they focused only on either the self-reported
447 or clinically ascertained phenotype in the UKBB, meaning some controls plausibly would have
448 had pneumonia, and thus, decreasing power. Moreover, the effective sample sizes (N_{eff}) of
449 these UKBB GWAS were markedly smaller than ours (177749 in the current discovery meta-
450 analysis versus 25915 and 39246, respectively).
451
452 We also considered two very recent smaller sample-size pneumonia GWAS without publicly
453 available summary statistics to see if we could replicate their findings. Firstly, Chen *et al.*
454 performed a GWAS of pneumonia susceptibility and severity in the Vanderbilt University
455 Biobank (BioVU, N_{Case} = 8889, $N_{Controls}$ = 60,767, N_{eff} = 31019) , European ancestry cohort)[44].
456 They found that a genome-wide significant common signal in Europeans associated with
457 pneumonia severity, with the lead SNP rs10786398 nominally associated in our meta-analysis:
458 β = -0.029, SE = 0.001, P = 2.5 x 10^{-4}, whilst we were unable to replicate the significant rare-
459 variant association signal from that study as the variant was not available in our analyses.
460 Moreover, a meta-analysis of a smaller previous FinnGen release and ICD-10 (N_{eff} = 94584)
461 derived pneumonia in the UKBB found two genome-wide significant index SNPs in the
462 15q15.1 region that were directionally consistent in our analyses, although not statistically
463 significant, with a trend observed for rs76474922: β = 0.025, SE = 0.01, P = 0.08 [45]. The SNP-

464 based heritability estimate from that study also closely mirrored ours (3.3% on the liability
465 scale), supporting the reliability of this study's estimate in a larger sample.
466
467 **Gene and gene-set association further supports a role for mucin biology in pneumonia**
468 We performed gene and gene-set association to investigate associations with pneumonia
469 beyond univariable SNP-phenotype relationships (Supplementary Tables 5,6). Six genes
470 outside of the MHC region were significant in the meta-analysis after the application of
471 multiple-testing correction (*MUC5AC*, *MUC5B*, *DUPD1*, *SAMD8*, *DUSP13*, and *TOX*), all of
472 which were within genome-wide significant loci except for the *TOX* gene (P = 1.26 x 10^{-6}),
473 which plays a role in T cell persistence during response to a pathogen[46,47]. Gene-set association
474 revealed a single gene-set for which its member genes were enriched with pneumonia
475 associated common variation relative to all other genes tested: *Termination of O-glycan*
476 *biosynthesis* – β = 0.89, SE = 0.21, P = 1.05 x 10^{-5}, q = 0.01. The strongest gene-based signal
477 in this pathway was accounted for by two mucin genes that span part of the genome-wide
478 significant loci on chromosome 11 (*MUC5AC, MUC2*), whilst there were four other mucin
479 genes within this set that displayed a nominal gene-based association (P < 0.05) outside that
480 region (*MUC15*, *MUC16*, *MUC12*, and *MUC17*). The signal from this gene-set remained
481 relatively robust upon using a more conservative definition of the genic boundaries for SNP to
482 gene annotation during gene-based association: β = 0.66, SE = 0.19, P = 3.04 x 10^{-4}. Rare
483 variants were then subjected to gene-based association by leveraging the properties of the
484 Cauchy distribution, such that covariance between P values did not need to be estimated. No
485 genes surpassed Bonferroni correction, considering genes with at least two rare variants. The
486 most significant gene found upon testing all genic rare variants was *ZNF19*, P = 6.3 x 10^{-5},
487 whilst *FREM1* was the top gene (P = 8.16 x 10^{-4}) considering variants annotated as exonic only
488 (Supplementary Tables 7,8). Furthermore, we utilised the gene-based results to construct a
489 competitive rare variant gene-set association model and tested the same gene-sets as in the
490 common variant analyses (Supplementary Tables 9,10). While there were no gene-sets that
491 survived multiple-testing correction utilising all genic rare variants or those with only exonic
492 annotated sites, we found some support for B lymphocyte antigen response in the rare variant
493 architecture of pneumonia, as the most significant association from the rare variant model was
494 with the *B cell antigen receptor* pathway - β = 0.59, SE = 0.19, P = 7.7 x 10^{-4}. Interestingly,
495 there was also a nominal rare variant signal amongst pathways related to carbohydrate
496 metabolism (*Metabolism of carbohydrates* – P = 6.22 x 10^{-3}, *Glycosaminoglycan degradation*

497 – $P = 0.02$) and glycosylation (*N-glycan biosynthesis* – $P = 0.01$), although these results must
498 be interpreted cautiously given, they do not survive multiple testing correction.
499
500 A transcriptome-wide association study was then undertaken to identify genes for which
501 genetically predicted expression was correlated with pneumonia susceptibility. We selected
502 SNP weights from three tissues which are plausibly biologically relevant to pneumonia
503 pathophysiology: lung, whole blood, and spleen. After applying Bonferroni correction to the
504 number of tests within each tissue outside the MHC individually, significant correlation was
505 observed between decreased predicted expression of *VDAC2* and pneumonia ($Z = -4.39$, $P =$
506 1.15×10^{-5}, Supplementary Table 11) using spleen tissue as the prediction model. The
507 association between *VDAC2* and pneumonia was also supported by SNP weights from the lung
508 and whole blood, although these did not surpass the Bonferroni threshold: $P_{\text{Lung}} = 5.52 \times 10^{-4}$,
509 $P_{\text{Whole blood}} = 9.97 \times 10^{-4}$. We tested a related, but distinct hypothesis by assessing evidence for
510 colocalisation between the GWAS signal spanning *VDAC2* and the SNP weights from the three
511 tissues utilised to construct the model of genetically predicted *VDAC2* expression.
512 Colocalisation assumes a biologically conservative parameter of a single shared causal variant
513 that underlies the relationship between *VDAC2* expression and pneumonia. We observed
514 heterogeneity between the three tissues, with moderately strong evidence of colocalisation
515 between *VDAC2* expression and SNP weights from whole blood ($PP_{\text{H4}} = 0.848$), however,
516 using lung and spleen expression SNP weights there was no strong evidence ($PP > 0.8$) for any
517 of the five colocalisation hypotheses. In lung, there was evidence for an association between
518 *VDAC2* lung expression SNP weights and pneumonia ($PP_{\text{H3}} = 0.568$, $PP_{\text{H4}} = 0.363$), although
519 we were not able to clearly determine whether there were two independent SNPs driving the
520 association (H3) or a shared variant (H4). Interestingly, there was moderate support in the
521 model leveraging the spleen SNP expression weights that this signal was only associated with
522 pneumonia and not *VDAC2* expression ($PP_{\text{H2}} = 0.643$), which could be driven by the spleen
523 model of genetically regulated expression being somewhat less predictive ($R^2 = 0.038$, best
524 linear unbiased prediction), than in blood ($R^2 = 0.1$, LASSO) and lung ($R^2 = 0.083$, elastic net),
525 respectively. Probabilistic finemapping of the marginal TWAS Z scores in the *VDAC2* region
526 was then undertaken using a multi-tissue panel to assess evidence for whether *VDAC2* is the
527 causal gene in this region. This locus was dense with genes, with 26 unique genes within the
528 90% credible set of causal genes. There was moderate evidence that *VDAC2* was the most
529 probable causal gene at this locus given it had the largest absolute TWAS Z, the highest *PIP*
530 for an individual model from the adrenal gland ($PIP = 0.279$), and a relatively large cumulative

531 *PIP* for all 17 *VDAC2* models derived a variety of tissues that were finemapped ($PIP_{\text{Cumulative}}$
532 = 0.683). Further investigation is thus needed to refine this locus.
533
534 There were a number of other genes that trended towards surviving multiple-testing correction
535 in spleen and the other two tissues – including, *PLD4* in spleen and *STPG1* in lung. We
536 subjected genes that trended towards multiple testing correction (two orders of magnitude
537 above the Bonferroni threshold) to gene-set overrepresentation analysis to identify gene
538 ontologies enriched for these genes, with *immune system process* and *immune response*
539 overrepresented after multiple-testing correction, supporting the biological relevance of this
540 signal (Supplementary Table 12). For instance, downregulation of tumour necrosis factor
541 receptor gene *TNFRS19* in lung trended towards correlation with pneumonia, $Z = -3.44$, $P =$
542 5.78×10^{-4}.
543
544 **Pneumonia displays genetic correlation with clinically significant phenotypes**
545 We estimated genetic correlation between pneumonia and 180 GWAS using LDSR, with a
546 significant non-zero estimate of genetic correlation obtained for twenty phenotypes after the
547 application of multiple testing correction ($P < 2.78 \times 10^{-4}$, Supplementary Table 13, Fig. 2).
548 Interestingly, the most significant genetic correlation was found between pneumonia and
549 insomnia ($r_g = 0.496$, $SE = 0.075$, $P = 3.55 \times 10^{-11}$), which supports previous observational data
550 that insomnia and reduced sleep duration increased the risk of developing pneumonia[48,49]. In
551 addition, we uncovered significant genetic correlation with other clinically interesting
552 phenotypes including forced vital capacity ($r_g = -0.215$, $SE = 0.0361$, $P = 2.62 \times 10^{-9}$), obesity
553 ($r_g = 0.3023$, $SE = 0.0466$, $P = 9.15 \times 10^{-11}$), and HDL cholesterol ($r_g = -0.2876$, $SE = 0.0664$,
554 $P = 1.48 \times 10^{-5}$).

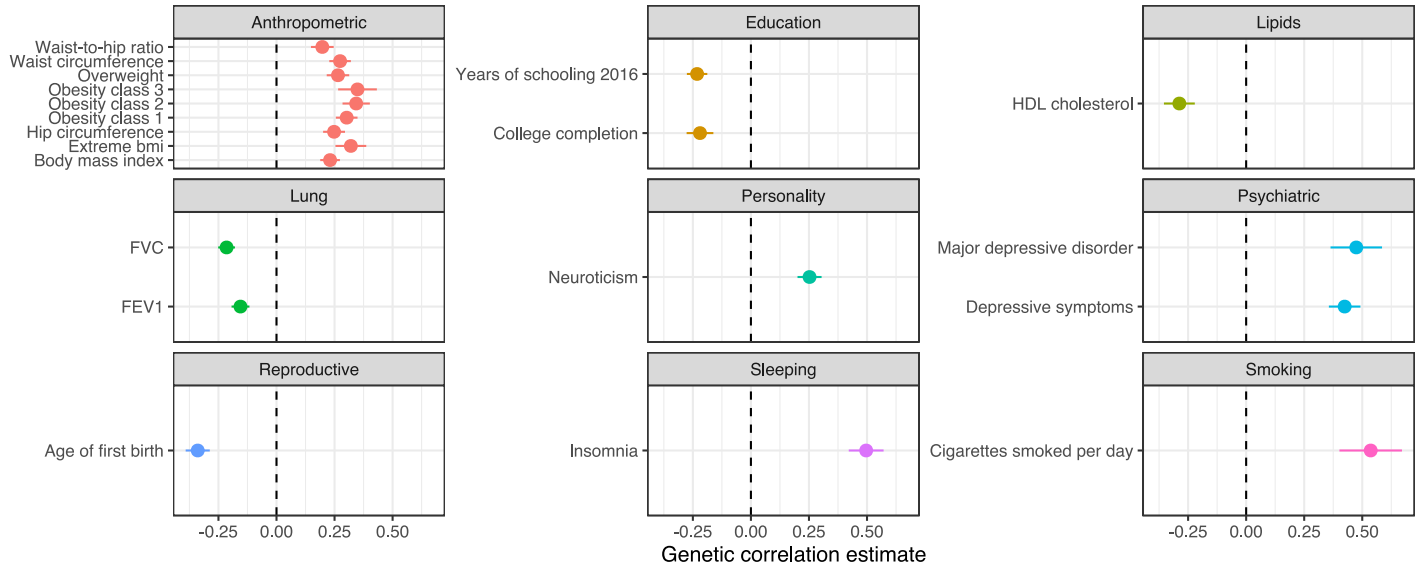

Figure 2. Estimates of genetic correlation between pneumonia and a panel of GWAS that survive multiple testing correction. Each panel of the forest plot is the estimate of genetic correlation by LD score regression (+/- its standard error, denoted by the error bars). The dotted lines represent a genetic correlation of zero. Panels were grouped by the phenotypic category of the trait subjected to LDSR.

A latent causal variable (LCV) model was then constructed for the most significantly correlated trait-pairs from each phenotypic category that comprised the 180 GWAS tested for genetic correlation. The LCV approach leverages the bivariate effect size distribution of SNPs in two GWAS and their LD scores to estimate a genetic causality proportion (GCP), such that, evidence of partial genetic causality can be distinguished from genetic correlation. We found strong evidence ($|\widehat{GCP}| > 0.6$) for partial genetic causality of cigarettes per day and HDL on pneumonia. Both posterior mean GCP estimates were significantly different from zero, however, the estimate of HDL → pneumonia ($\widehat{GCP} = 0.758$, $SE = 0.159$, $P = 2.20 \times 10^{-11}$) was more precise than that of cigarettes per day → pneumonia ($\widehat{GCP} = 0.713$, $SE = 0.225$, $P = 3.51 \times 10^{-3}$). The magnitude of the potential causal relationship between HDL and pneumonia was further investigated using mendelian randomisation (MR). Given the biological overlap between the genetic architecture of HDL and other lipid classes, we constructed a multivariable MR model that conditioned HDL instrumental variables on their association with LDL cholesterol and triglycerides, obtaining the SNP-exposure estimates

578 from the Willer *et al.* global lipids genetics consortium paper , as has been outlined elsewhere
579 [29,50]. There was no evidence of a causal effect of HDL ($P = 0.65$) or LDL ($P = 0.47$)
580 conditioned on the remaining lipid classes, although there was nominal evidence of a risk
581 increasing effect of triglycerides on pneumonia – $\beta = 0.058$, $SE = 0.028$, $P = 0.035$. These
582 data highlight the complexities of distinguishing between confounding pleiotropy and
583 evidence for causal relationships, with further work needed to resolve whether the
584 directionally disproportionate variant effect sizes for HDL → pneumonia captured by the
585 LCV model represent a true evidence for a causal relationship or whether other factors like
586 triglycerides may explain this relationship. In addition, the effect of other confounders like
587 BMI on these relationships cannot also be ruled out, although BMI did not show evidence of
588 a causal effect in the LCV model.
589
590 **Opportunities for drug repurposing by leveraging the genetic architecture of pneumonia**
591 We sought to interrogate the pneumonia GWAS to propose novel drug repurposing candidates
592 that could be useful to treat patients diagnosed with pneumonia more effectively. Firstly, we
593 utilised a very liberal approach which identified genes that were targeted by approved drugs
594 outside the MHC region physically mapped to loci associated with pneumonia at a minimum
595 of a suggestive significance threshold ($P < 1 \times 10^{-5}$). There were five such genes that displayed
596 a high confidence interaction with an approved pharmacological agent with a known
597 mechanism of action – *IL6R*, *SCNN1A*, *ATP2B1*, *ERBB2*, and *STAT5B*). For instance,
598 Tocilizumab is a monoclonal antibody that targets *IL6R* which has been suggested as a
599 repurposing opportunity to use for severe illness following SARS-CoV2 infection, although
600 results from randomised controlled trials have been mixed in terms of efficacy[51]. We examined
601 these genes in the TWAS analyses, however, only *IL6R* was significantly *cis*-heritable in one
602 of the three tissues we utilised. Interestingly, there was a trend towards a correlation between
603 downregulation of *IL6R* and increased odds of pneumonia, which would not support the use of
604 anti-IL-6 receptor agents like tocilizumab – $Z = -3.148$, $P = 1.64 \times 10^{-3}$. In contrast, the lead
605 SNP and odds increasing allele of the *IL6R* locus in this GWAS has been associated with
606 increased *IL6R* levels in a protein quantitative trait loci study (pQTL), which would support
607 the efficacy of tocilizumab. We caution that the pQTL signal is in high LD with a missense
608 variant (rs2228145), and thus, antigen binding affinity may be altered to create an artefactual
609 pQTL association. These antigen-binding affinity related effects require further investigation,
610 particularly in light of the phenomenon of the non-synonymous rs2228415 C allele displaying
611 correlation with increased protein abundance from the pQTL study[52] but with decreased

612 expression via RNAseq derived eQTL estimates from whole blood by GTEx, along with
613 decreased CRP levels in the UK biobank, a well-characterised biomarker of IL-6 receptor (IL-
614 6R) inhibition. Previous functional analyses of the rs2228145 non-synonymous allele have
615 demonstrated that it likely impairs IL6 signalling, with increased expression of soluble
616 circulating IL-6R but downregulation of the membrane bound isoform[53]. As a result, we
617 conclude that based on the genetic association alone that the anti-inflammatory effect of IL-6R
618 blockade may have a risk-increasing impact on pneumonia, although further work is required
619 to evaluate tocilizumab as a potential repurposing opportunity, particularly as its efficacy
620 would likely be dependent on its temporal application in the clinical course of the disease.
621
622 A panel of 50 metabolites and blood cell count phenotypes from the UK biobank (UKBB) with
623 moderate to high confidence SNP-based heritability estimates were then tested for genetic
624 correlation with pneumonia (Supplementary Table 14). The concept underlying this is that if
625 there is evidence of a relationship between a biochemical trait and pneumonia, then a drug
626 which modulates that trait in a risk-decreasing direction could be clinically useful, and thus,
627 repurposed for pneumonia. We found 13 biochemical traits from the UKBB panel that were
628 correlated with pneumonia after multiple-testing correction (Supplementary Table 15). The
629 most significant correlation was a positive genetic correlation with triglycerides, followed by
630 a positive correlation with glycaeted haemoglobin (HbA1c), which is interesting given
631 previous evidence that hyperglycaemia has a deleterious effect on lung function[27,54]. The
632 correlation between HbA1c and pneumonia may not be necessarily driven by glycaemic
633 biology, particularly as HbA1c is strongly influenced by haematological factors, although we
634 did observe weak evidence for a positive correlation between glucose and pneumonia that does
635 not survive multiple testing correction ($P = 0.01$, Supplementary Table 15). It should be noted
636 that this UKBB sample is a larger sample size than the triglyceride GWAS subjected to LDSR
637 in the broad LDhub GWAS panel from earlier in the manuscript, and thus, the estimate is more
638 significant in this analysis. In addition, the HDL GWAS from the UKBB was not included due
639 to anomalous estimates of large standard error when considering its heritability estimate
640 (Supplementary Methods). There was only very weak evidence from the LCV model for a
641 potential causal influence of triglycerides on pneumonia ($\widehat{GCP} = 0.465$, $SE = 0.226$, $P = 0.052$,
642 Figure 3a), although this broadly supports the results of the lipid multivariable MR described
643 earlier in the manuscript that provided nominal evidence of a deleterious impact of increased
644 triglycerides. We attempted to replicate the earlier multivariable MR results using the LDL,

645 HDL, and triglyceride GWAS from the UK biobank as the exposure traits rather than the Willer
646 *et al*. global lipids genetics consortium GWAS, with an analogous result that demonstrated an
647 odds-increasing effect of triglycerides but a non-significant effect of LDL or HDL cholesterol
648 (Supplementary Table 16). We followed this up by estimating a univariable estimate of
649 triglycerides → pneumonia, with a 5.4% mean increase in the odds of pneumonia per standard
650 deviation increase in triglycerides across the five MR methods utilised (Supplementary
651 Methods, Supplementary Table 17). The causal estimate was only statistically significant in
652 the case of the two IVW estimators: OR = 1.056 [95% CI: 1.01, 1.104], P = 0.017 (IVW
653 multiplicative random effects), however, the remaining models had relatively consistent point
654 estimates of the effect of triglycerides on pneumonia (Figure 3b). There was some nominal
655 evidence of heterogeneity amongst IV exposure-outcome estimates (Q = 212.51, df = 168, P =
656 0.01), however, the Egger intercept was not significantly different from – thus, we observed
657 no direct statistical evidence of confounding pleiotropy. As a result, these data suggest a
658 potential repurposing opportunity for drugs prescribed for hypertriglyceridemia, such as statins
659 and fibrates, with the caveat that the MR and LCV models from this study provide only
660 relatively weak to moderate support, particularly as the mean posterior GCP estimate was low,
661 and thus, genetic correlation could contaminate the MR estimate.
662
663 The remaining LCV models for biochemical traits genetically correlated with pneumonia did
664 not indicate any strong evidence of partial genetic causality, with the exception of a putative
665 effect of gamma-glutamyltransferase (GGT) on pneumonia that approximately reached the
666 threshold for a strong point estimate of the GCP - $\widehat{GCP}$ = 0.59, SE = 0.212, P = 1.08 x 10^{-4}.
667 GGT is an enzyme that is commonly characterised as a biomarker of liver dysfunction, with
668 some evidence of an immunological role for this enzyme, as well as its involvement in alveolar
669 gas exchange. We further investigated this putative causal relationship by leveraging 207
670 independent SNPs associated with GGT ($P < 5 \times 10^{-8}$) in the UK biobank as IVs – approximated
671 variance explained by IVs = 6.47%, F-statistic = 114.91. The five MR models implemented in
672 this study yielded a roughly similar effect size per SD increase in GGT that increased the odds
673 of pneumonia (mean pneumonia OR per SD GGT increase = 1.055, Supplementary Table 18).
674 However, the estimates were not statistically significant, with the exception of the weighted
675 median model (OR = 1.087 [95% CI: 1.01, 1.17], P = 0.025). There was evidence of
676 heterogeneity amongst the IV exposure-outcome effects, which may be indicative of
677 confounding pleiotropy (Q = 301.87, df = 206, P = 1.501 x 10^{-5}), although given the large

number of IVs observed heterogeneity is not a surprising phenomenon. Importantly, there was no statistical evidence of pleiotropy from the intercept of the MR egger model. We caution that statistical approaches to assess pleiotropy do not and cannot rule out a confounding influence on the MR estimate, and detailed biological annotation of the IVs would be warranted to investigate this further. In summary, there may be a causal relationship between GGT and increased odds of pneumonia which could support inhibition of this enzyme as a treatment target, with several GGT inhibitors under active development and explored for use in respiratory illness[55,56].

Furthermore, we compared the MR estimate of the effect of a standard deviation increase in GGT and triglyceride concentration on the odds of pneumonia to an observational estimate from the UK biobank sample (Supplementary Methods). We found that the observational association between a standard deviation increase in triglyceride concentration and pneumonia was analogous to the univariable and multivariable MR estimates (OR = 1.059 [95% CI: 1.042, 1.076], $P = 2 \times 10^{-12}$), whilst the observed association between GGT and pneumonia was stronger than the MR estimate, with each standard deviation associated with a 13.54% [95% CI: 12.43%, 14.56%] increase in the odds of pneumonia amongst UK biobank participants. Interestingly, these associations were also consistent amongst individuals in the UK biobank with relatively lower risk of pneumonia, that is, non-smoking females aged 45 or younger at time of assessment – triglycerides: OR = 1.335 [95% CI: 1.13, 1.555], $P = 2.67 \times 10^{-4}$, GGT: OR = 1.354 [95% CI: 1.161, 1.553], $P = 2.75 \times 10^{-5}$. These variables are extremely heterogeneous and there are many potential confounders of the observed effect sizes, however, it supports the inferred relationship from the LCV and MR models.

a

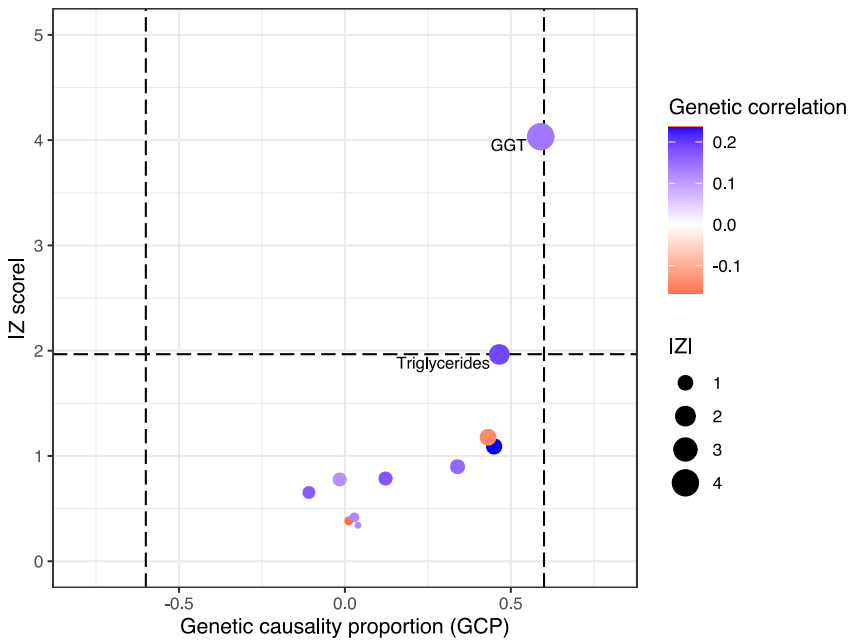
GGT
Triglycerides
IZ score|
Genetic causality proportion (GCP)
Genetic correlation
0.2
0.1
0.0
-0.1
|Z|
1
2
3
4

b

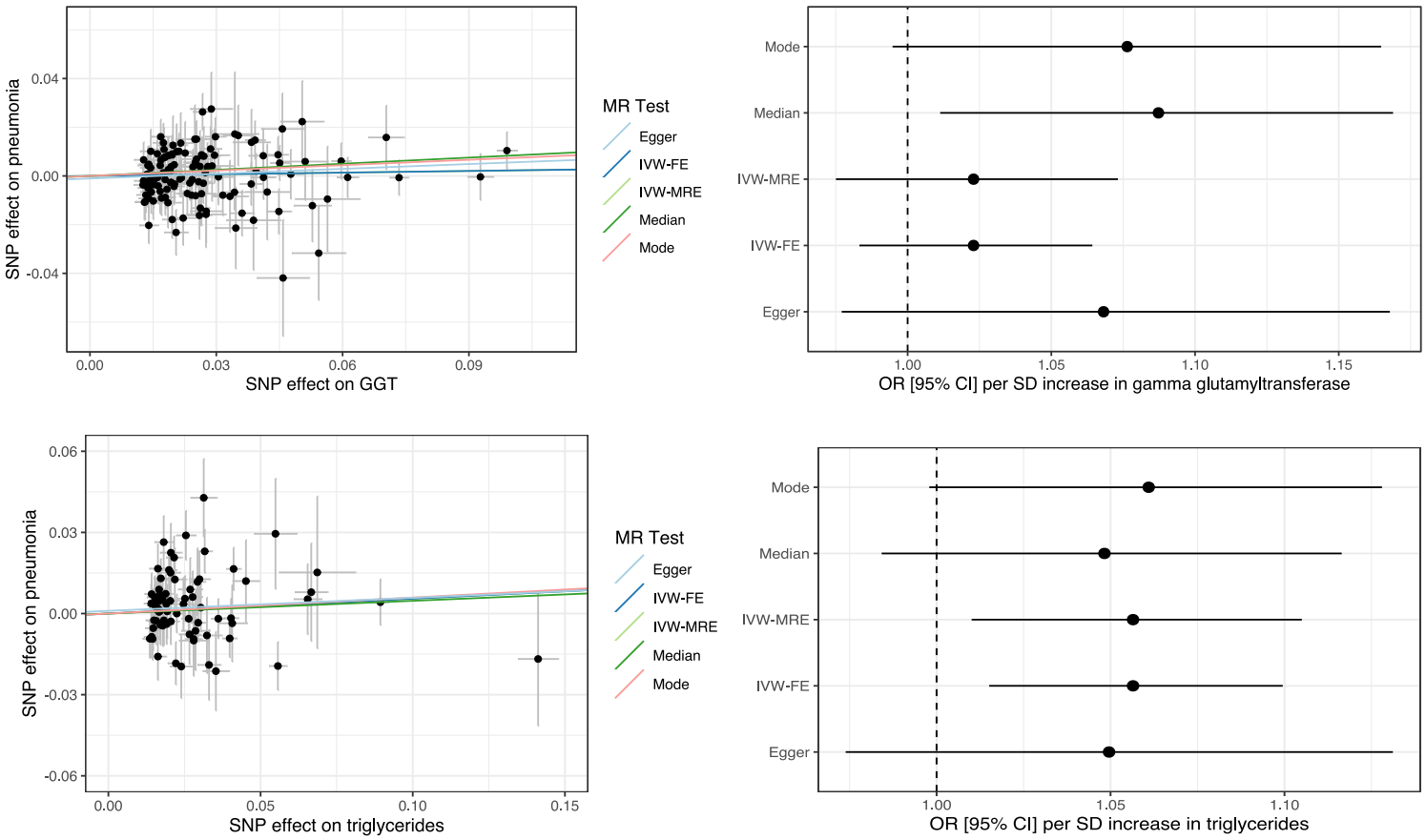
SNP effect on pneumonia
SNP effect on GGT
MR Test
Egger
IVW-FE
IVW-MRE
Median
Mode
OR [95% CI] per SD increase in gamma glutamyltransferase
SNP effect on triglycerides
OR [95% CI] per SD increase in triglycerides

718 **Figure 3. Investigating the potential utility of modulating biochemical traits as**
719 **drug repurposing opportunities for pneumonia.** (**a**) Latent causal variable models
720 constructed between genetically correlated trait pairs after Bonferroni correction. Each
721 point represents the genetic causality proportion, with the *y* axis denoting the precision
722 of the GCP estimate, that is, its *Z* score. The genetic correlation estimate between the
723 two traits was utilised to shade the points, with the larger points also indicative of a
724 larger GCP *Z* score. A positive GCP estimate is indicative of partial genetic causality
725 of the biochemical trait → pneumonia, whilst a negative estimate represents the
726 converse. (**b**) A Mendelian randomisation (MR) analysis of the effect of genetically
727 proxied gamma glutamyl-transferase (GGT) and triglycerides on the odds of
728 pneumonia. The scatter plot visualises the effect of each instrumental variable SNP on
729 GGT or triglycerides verses its effect on pneumonia, with the regression trend line the
730 MR estimate from each of the five models implemented. Similarly, the forest plot
731 indicates the pneumonia odds ratio for each of the MR models, with the error bar
732 indicative of the 95% confidence intervals. The MR models were as follows: mode =
733 weighted mode estimator, median = weighted median estimator, IVW-FE = inverse-
734 variance weighted estimator with fixed effects, IVW-MRE = inverse-variance weighted
735 estimator with multiplicative random effects, Egger = MR-Egger regression.
736
737
738 **Precision drug repurposing to treat pneumonia**
739
740 We implemented the *pharmagenic enrichment score* (PES) approach to identify drug
741 repurposing candidates that could be targeted more precisely based on genetic risk[27,37]. Briefly,
742 the PES is a genetic risk score specifically within a biological pathway that is targeted by
743 approved drugs. The concept underlying the PES is that individuals with elevated genetic risk
744 within a particular druggable set of genes may benefit from a pharmacological agent that
745 modulates the pathway in question. Firstly, we identified five druggable pathways that
746 displayed an enrichment of the common variant genetic architecture of pneumonia at one of
747 four *P*-value thresholds for the inclusion of variants in the model (FDR < 0.05, Table 2,
748 Supplementary Table 19, Supplementary Methods). These included two complement-related
749 pathways, *p53 signalling*, and *bile acid metabolism*.
750

751 **Table 2. Candidate druggable gene-sets that could be utilised to calculate *pharmagenic***
752 ***enrichment scores***

PES gene-set	P_T[1]	P	Example drug/nutraceutical
P53 signalling pathway	0.05	2.13×10^{-8}	Fostamatinib
Lectin induced complement pathway	0.05	2.98×10^{-8}	Human immunoglobulin
Complement pathway	0.05	6.81×10^{-8}	Zinc
Bile acid metabolism	0.005	1×10^{-6}	Atorvastatin
RIG-I-like receptor signalling pathway	0.005	1.58×10^{-5}	Etanercept

753 [1]P_T = P value threshold for variant inclusion in the model
754
755 There were a number of diverse compounds that targeted these pathways, with compounds
756 identified as repurposing candidates through testing whether there was a statistically significant
757 overrepresentation of their targets in the gene-set, along with high confidence single drug-gene
758 interactions (Supplementary Tables 20,21). For instance, targets of the micronutrient zinc were
759 overrepresented amongst genes in the *Complement pathway* gene-set, supporting previous
760 evidence that zinc can modulate complement activation [57,58].
761
762 *Characteristics of pneumonia pharmagenic enrichment scores*
763
764 We investigated the properties of these five scores in the UKBB cohort. Interestingly, there
765 were no large correlations (all $r < 0.07$) between the PES and a genome-wide polygenic risk
766 score for pneumonia, which supports our hypothesis that pathway-based risk scores may
767 provide novel biological insights that are not encompassed by PRS constructed from variants
768 throughout the genome. Both the genome wide PRS and the PES profiles were not significantly
769 associated with pneumonia diagnosis (self-reported/clinically ascertained or clinically
770 ascertained only, Supplementary Tables 22,23, Supplementary Methods). This is perhaps not
771 surprising given the low SNP heritability of pneumonia and the heterogeneity of the phenotype
772 – however, we believe this does not preclude the relevance of PES at an individual level. For
773 instance, given the putative relationship between hypertriglyceridemia and increased odds of
774 pneumonia, as supported by this study, we tested the relationship between the pneumonia *Bile*
775 *acid metabolism* PES and measured triglycerides in the UKBB. There was a small but
776 significant positive correlation between the PES and triglyceride concentration – $\beta = 0.01$, SE
777 $= 0.002$, $P = 1.69 \times 10^{-4}$, which was significant even after adjusting for statin use or using
778 triglyceride values as the outcome variable winsorized at three standard deviations above the

779 mean to guard against an excessive influence of outliers (β = 0.01, *SE* = 0.002, *P* = 1.43 x 10^{-}
780 ^{4}). This relationship with triglycerides was not seen using genome wide PRS (β = 1.57 x 10^{-4},
781 *SE* = 0.002, *P* = 0.93).
782
783 *Associations between pneumonia pharmagenic enrichment scores and host susceptibility to*
784 *infection*
785
786 The relationship between PES, as a function of host genetic susceptibility to pneumonia, and
787 antibody response to infection was then assessed in a subset of the UKBB with these data
788 available and passing our genotyping QC thresholds (N = 6443). We implemented these
789 analyses given the host-immune response is directly relevant to pneumonia and if the PES
790 displays distinct correlations with antibody response compared to genome-wide pneumonia
791 PRS, it would emphasise the potential biological utility of the PES framework. Firstly, we
792 tested the association between each PES and antibody response to 28 antigens amongst
793 individuals with detectable levels of antibodies for 14 infections (seroreactivity, Fig. 4c,
794 Supplementary Table 24). The strongest relationship between a PES profile and seroreactivity
795 was a positive correlation between the *Complement pathway* PES and IgG response to the
796 major capsid protein VP1 of the BK polyomavirus, with each SD increase in the PES associated
797 with a 0.05 (0.01) SD increase in antibody response, *P* = 4.1 x 10^{-4}, which trended towards
798 surviving multiple testing correction (*q* = 0.07). There was no association between genome
799 wide PRS and IgG mediated response to this antigen. There were other nominally significant
800 correlations observed (Fig. 4a), with most of these correlations positive and potentially
801 indicative of an increased immune response. In addition, susceptibility to infection
802 (seropositivity) was also investigated (Supplementary Table 25). For instance, a nominal
803 association uncovered between *RIG-I-like receptor signalling pathway* and decreased odds of
804 herpes simplex virus-1 infection (OR = 0.93 per SD in score [95% CI: 0.87, 0.98], *P* = 4 x 10^{-}
805 ^{3}), whilst *Complement pathway* PES was nominally associated with increased odds of positive
806 *H. pylori* serostatus - OR = 1.07 per SD in score [95% CI: 1.01, 1.12], *P* = 0.02.
807
808
809
810
811
812

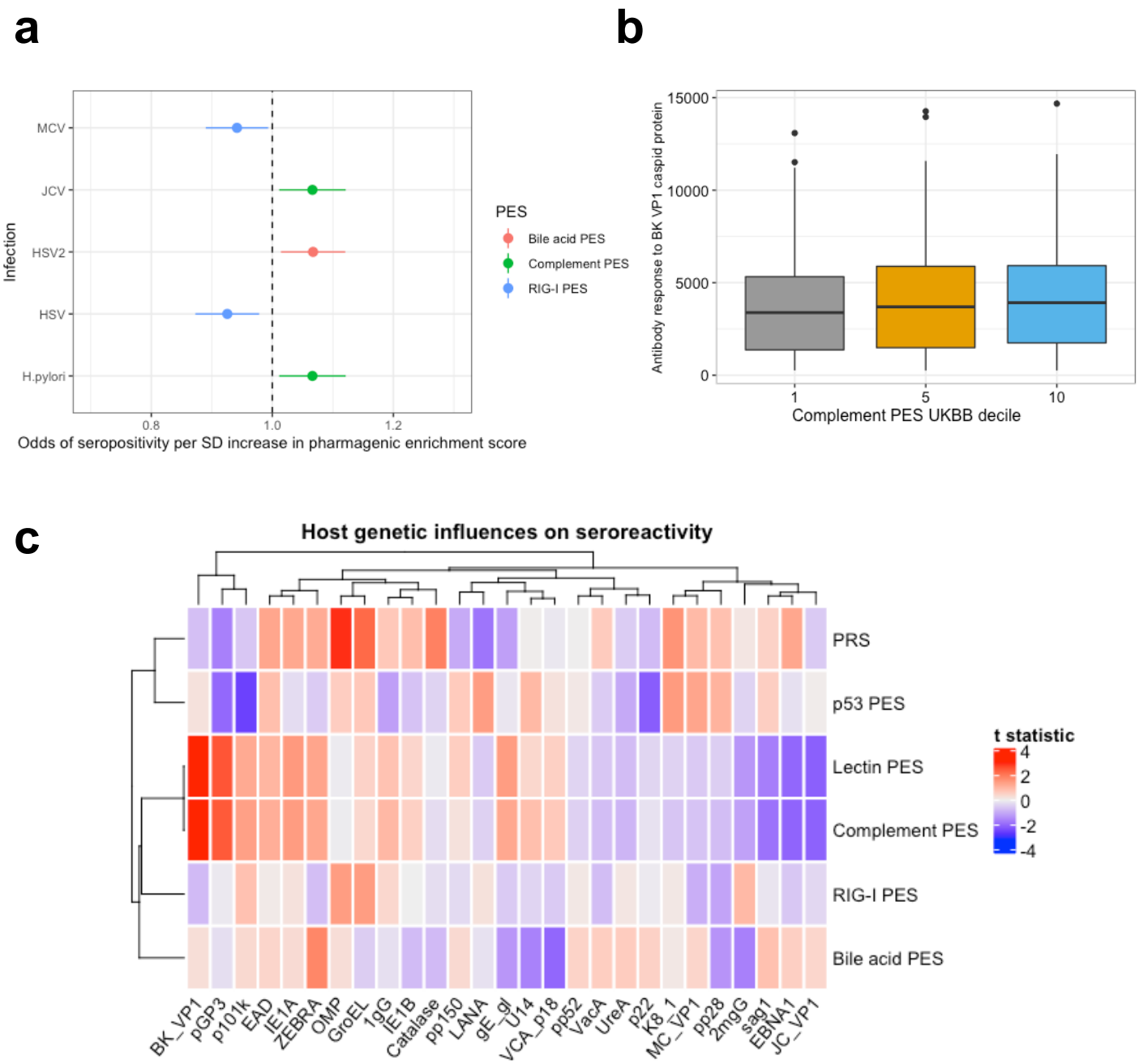

Figure 4. The relationship between host genetics pneumonia pathway based *pharmagenic enrichment scores* and antibody response. (**a**) Nominally significant associations between pneumonia PES and seropositivity as a binary variable. The forest plot denotes the odds ratio of each infection serostatus (error bars represent 95% confidence intervals) per SD increase in the PES tested. The infections abbreviated are as follows: MCV = Merkel Cell Polyomavirus, JCV = Human Polyomavirus JCV, HSV = herpes simplex virus 1, HSV2 = herpes simplex virus 2, *H. pylori* = Helicobacter pylori. (**b**) IgG response (mean fluorescence intensity) to the major capsid protein VP1

847 of the BK polyomavirus in the 10th percentile (1st decile, denoted 1), 50th percentile (5th
848 decile, denoted 5), and 90th percentile (10th decile, denoted 10) of the complement
849 pathway PES amongst the genotyped subset of the UKBB subjected to antibody
850 screening included in our analyses. (**c**) Heatmap of the regression *t* statistic
851 (beta/standard error) for the correlation between each PES and PRS with respective IgG
852 response to antigens amongst individuals seropositive for that infection. Hierarchical
853 clustering was applied to the rows and columns using Pearson's correlation distance.
854

855 **DISCUSSION**

856 In this study, we uncovered the first significant association signals for lifetime pneumonia
857 susceptibility outside of the MHC region. Interestingly, there was also a novel low frequency
858 variant in the MHC itself which reached genome-wide significant that confers a relatively large
859 (~ 59%) increase in the odds of pneumonia, reflecting the immense heterogeneity spanned
860 within this region. Further analyses of the MHC signal are warranted, particularly to
861 deconvolve specific HLA types that may contribute to pneumonia susceptibility and
862 progression. Each of the loci beyond the MHC identified this study were relatively complex,
863 although we were able to derive a 95% credible set for the most significant non-MHC locus on
864 chromosome 11 that implicated the mucin gene *MUC5AC*. It should be noted that our fine-
865 mapping approach is relatively biologically naïve as it assumes a single causal variant, and
866 thus, the involvement of other genes remains unclear. *MUC5AC* is an interesting candidate
867 given that it has been previously implicated in the pathogenesis of respiratory illness and the
868 role of mucins in physical defence against pathogens via mucociliary clearance[59]. This heavily
869 glycosylated protein is lowly expressed in normal respiratory epithelium, however, is
870 upregulated upon in response to perturbagens, such as viral infection[60,61]. We posit that
871 upregulation of *MUC5AC* may be deleterious in the context of pneumonia given recent
872 evidence that this protein can enhance airway inflammation induced by viral infection[62],
873 although dissection of the mechanisms of variants in this locus are warranted, particularly given
874 the apparent discordant relationship of this signal we observed on the odds on asthma.
875 Interestingly, there are some preliminary data that suggests *MUC5AC* is upregulated in the
876 airway mucus of patients with severe COVID-19, although these studies were conducted using
877 small sample sizes[63,64]. There was also evidence of a more expansive polygenic signal amongst
878 mucin and beta-galactoside/N-acetylgalactosaminide genes in the *termination of O-glycan*
879 *biosynthesis pathway*, whereby sialic acid residues conjugated to mucins can terminate O-
880 glycan biosynthesis[65]. Interestingly, therapies specifically targeting mucin-linked O-

881 glycosylation are now under active development, including a recently proposed hexosamine
882 analog that demonstrated potent inhibition of O-glycan biosynthesis and downregulation of
883 neutrophil infiltration in rodents[66].
884
885 Drug repurposing is an attractive downstream application for GWAS, and we demonstrate its
886 potential utility for pneumonia through three distinct methods. Causal inference between
887 biochemical traits and pneumonia may provide repositioning opportunities along with a greater
888 understanding of pathological mechanisms in the disorder. For instance, we reveal evidence to
889 suggest a potential protective effect of HDL cholesterol and a deleterious impact of elevated
890 triglycerides on the odds of pneumonia. These data support observational data that lower
891 baseline HDL and elevated triglycerides have risk-increasing properties for pneumonia[67–69], .
892 We emphasise that our data only provided weak to moderate support for a causal influence of
893 lipid abundance on pneumonia, and replicated, well-powered randomised controlled trials are
894 needed to definitively assess the suitability of lipid-modifying agents like statins. A key
895 limitation of proposing drug repurposing candidates for the phenotype as a singular entity is
896 that it ignores the inherent heterogeneity of pneumonia onset and clinical course. It has been
897 shown previously that individual genes supported by GWAS significantly increase the
898 likelihood of a candidate drug being successfully approved from the phase I stage [70], however,
899 the relevance of more expansive association signals relating to biological networks for
900 precision medicine remains unclear As a result, we sought to implement an approach which
901 seeks to target drug repositioning opportunities to those with elevated genetic risk within
902 pathways relevant to the compound (PES, one of the prioritised pathways for the construction
903 of a PES was the *Bile acid metabolism* gene-set, further supporting the relevance of compounds
904 that modulate cholesterol. In the UKBB cohort, we demonstrated that these scores were distinct
905 from genome-wide PRS, and thus, may offer biological insights that were missed by using a
906 genome-wide score. For example, the *Bile acid metabolism* PES was positively correlated with
907 triglyceride levels, whilst this was not observed for PRS. We caution that one cannot draw a
908 causal inference from this relationship. In addition, the putative relationship between PES and
909 IgG response to antigens is biologically relevant both in terms of increased and decreased
910 antibody response. One can conceptualise the phenotype of pneumonia as having a contribution
911 from increased likelihood of infection, but also an aberrant inflammatory response once
912 infected with a pathogen. The distinct signal observed with these IgG phenotypes for the
913 pathway-based PES compared to genome-wide PRS, therefore, further highlights the potential
914 utility of the PES framework. Further work is required to evaluate the suitability of compounds

915 that modulate the PES pathways of interest and to categorise drug repurposing candidates based
916 on their suitability for prevention and/or treatment of pneumonia. The key advantage of the
917 PES framework is that only individuals with relevant genetic background in a pathway of
918 interest would be prioritised for the respective repurposing candidate, which would be useful
919 given the polygenic nature of complex disorders. Detailed discussion of the strengths and
920 limitations of the PES methodology have been featured in previous publications[27,37].
921
922 There are a number of important limitations that should be considered in light of the pneumonia
923 GWAS itself and our drug repurposing analyses. Firstly, this GWAS was conducted using
924 samples from European ancestry as large, diverse, genotyped cohorts with pneumonia status
925 information are not yet available. It will be critical to translate findings related to host-genetic
926 influences on pneumonia that future efforts strive to collect trans-ancestral data, particularly
927 due to concerns about the portability of European GWAS signals and the advantages in
928 finemapping afforded by including multiple ancestries[71]. The SNP heritability for pneumonia
929 derived in this study was also relatively low, and it remains unclear how heterogeneity amongst
930 the phenotype definition of pneumonia may contribute to this. In other words, given that
931 pneumonia is caused by a variety of factors and may go undiagnosed in some individuals,
932 detailed phenotyping data would potentially assist in resolving the genetic architecture of this
933 disorder. For example, a GWAS on susceptibility verses pneumonia severity will likely reveal
934 different biological insights. This could also be aided by stratified analyses by age, given
935 pneumonia is more pervasive in the elderly. The putative drug repurposing candidates
936 suggested in this study must also be viewed in light of the low heritability of pneumonia and
937 need for clinical validation. Despite these challenges, we believe that further resolving the host-
938 genetic architecture of pneumonia will be invaluable to public health efforts to more effectively
939 prevent and manage the illness. In summary, we revealed novel genome-wide significant loci
940 associated with life-time pneumonia susceptibility beyond the MHC region. These data
941 provided some support for the potential utility of triglycerides and GGT as treatment targets
942 for pneumonia, however, randomised controlled trials are now required to establish the efficacy
943 of such interventions. Moreover, the *pharmagenic enrichment score* approach may provide a
944 precision medicine-based intervention for drug repurposing for pneumonia prophylaxis and
945 treatment given an individual's composition of genetic risk. The properties of these scores and
946 the prospects of integrating them with other clinical metrics warrants further research.
947
948

949 **DECLARATION OF INTERESTS**

950 W.R.R and M.J.C have filed a patent related to the use of the pharmagenic enrichment score
951 framework in complex disorders, the remaining authors declare no competing financial
952 interests.

953

954 **ACKNOWLEDGEMENTS**

955 We wish to acknowledge the participants and investigators of FinnGen study and the 23andMe
956 Inc. study from which these data were derived for the GWAS meta-analysis. In addition, his
957 research has been conducted using the UK Biobank Resource under the application 58432.
958 This study was supported by an NHMRC project grant (1147644). M.J.C. is supported by an
959 NHMRC Senior Research Fellowship (1121474).

960

961 **CONSORTIA**

962

963 **The 23andMe Research Team**

964 Michelle Agee[3], Babak Alipanahi[3], Robert K. Bell[3], Katarzyna Bryc[3], Sarah L. Elson[3], Pierre
965 Fontanillas[3], Nicholas A. Furlotte[3], Barry Hicks[3], David A. Hinds[3], Karen E. Huber[3], Ethan M.
966 Jewett[3], Yunxuan Jiang[3], Aaron Kleinman[3], Keng-Han Lin[3], Nadia K. Litterman[3], Jennifer C.
967 McCreight[3], Matthew H. McIntyre[3], Kimberly F. McManus[3], Joanna L. Mountain[3], Elizabeth
968 S. Noblin[3], Carrie A. M Northover[3], Steven J. Pitts[3], G. David Poznik[3], J. Fah
969 Sathirapongsasuti[3], Janie F. Shelton[3], Suyash Shringarpure[3], Chao Tian[3], Joyce Y. Tung[3],
970 Vladimir Vacic[3], Xin Wang[3] & Catherine H. Wilson[3].

971

972 **AUTHOR INFORMATION**

973

974 **School of Biomedical Sciences and Pharmacy, Faculty of Health and Medicine, The**
975 **University of Newcastle, Callaghan, NSW, 2308, Australia**
976 William R. Reay, Michael P. Geaghan, and Murray J. Cairns

977

978 **Hunter Medical Research Institute, Newcastle, NSW, 2305, Australia**
979 William R. Reay, Michael P. Geaghan, and Murray J. Cairns

980

981 **23andMe Inc., Sunnyvale, CA, 94086, United States of America**
982 The 23andMe Research Team

983 **WEB RESOURCES**

984 DGIdb v4.2.0 - https://www.dgidb.org/

985 FAVOR - http://favor.genohub.org/

986 FOCUS version July 24 2019 - https://github.com/bogdanlab/focus

987 FUMA v1.3.6 - https://fuma.ctglab.nl/

988 FUSION version May 29 2020 - https://github.com/gusevlab/fusion_twas

989 LCV version March 15 2019 - https://github.com/lukejoconnor/LCV

990 LDSR v1.0.1 - https://github.com/bulik/ldsc

991 MAGMA v.1.07b - https://ctg.cncr.nl/software/magma

992 METAL version March 2011 - https://genome.sph.umich.edu/wiki/METAL_Quick_Start

993 MR-PRESSO v1 - https://github.com/rondolab/MR-PRESSO/commits/master

994 mtCOJO (GCTA version 1.93.2 beta mac) -

995 https://cnsgenomics.com/software/gcta/#mtCOJO

996 PLINK2 v.2.00a3LM - https://www.cog-genomics.org/plink/2.0/

997 PRSice-2 v.2.3.3 (linux) - https://www.prsice.info/

998 TwoSampleMR v.0.5.5 - https://github.com/MRCIEU/TwoSampleMR

999 VEP GRCh37 release 101 August 2020 -

1000 https://grch37.ensembl.org/Homo_sapiens/Tools/VEP?db=core

1001 WebGestaltR v.4.0.2 - https://github.com/bzhanglab/WebGestaltR

1002

1003

1004 **DATA AND CODE AVAILABILITY**

1005 All data in this study are publicly available, summary statistics from 23andMe Inc. can be

1006 obtained upon application to the company. As per 23andMe data sharing policies, we are

1007 only able to release 10,000 SNPs from our meta-analysis, which we have made available on

1008 GitHub

1009 (https://github.com/Williamreay/Pneumonia_meta_GWAS_drug_repurposing/tree/master/Su

1010 mmary_statistics). The full GWAS summary statistics for the 23andMe discovery data set

1011 will be made available through 23andMe to qualified researchers under an agreement with

1012 23andMe that protects the privacy of the 23andMe participants.

1013 Researchers wishing to recapitulate our meta-analysis can apply for access for the 23andMe

1014 subset of the study (https://research.23andme.com/dataset-access/), and then meta-analyse

1015 with FinnGen release 3 summary statistics as described in our manuscript. Code utilised in

1016 this study is available also on GitHub -

1017 https://github.com/Williamreay/Pneumonia_meta_GWAS_drug_repurposing.

1018

1019

1020 **REFERENCES**

1021 1. Mackenzie, G. (2016). The definition and classification of pneumonia. Pneumonia
1022 (Nathan) *8*, 14.

1023 2. Restrepo, M.I., Faverio, P., and Anzueto, A. (2013). Long-term prognosis in community-
1024 acquired pneumonia. Curr Opin Infect Dis *26*, 151–158.

1025 3. McAllister, D.A., Liu, L., Shi, T., Chu, Y., Reed, C., Burrows, J., Adeloye, D., Rudan, I.,
1026 Black, R.E., Campbell, H., et al. (2019). Global, regional, and national estimates of
1027 pneumonia morbidity and mortality in children younger than 5 years between 2000 and 2015:
1028 a systematic analysis. Lancet Glob Health *7*, e47–e57.

1029 4. Obel, N., Christensen, K., Petersen, I., Sørensen, T.I.A., and Skytthe, A. (2010). Genetic
1030 and Environmental Influences on Risk of Death due to Infections Assessed in Danish Twins,
1031 1943–2001. American Journal of Epidemiology *171*, 1007–1013.

1032 5. Tian, C., Hromatka, B.S., Kiefer, A.K., Eriksson, N., Noble, S.M., Tung, J.Y., and Hinds,
1033 D.A. (2017). Genome-wide association and HLA region fine-mapping studies identify
1034 susceptibility loci for multiple common infections. Nat Commun *8*, 599.

1035 6. Willer, C.J., Li, Y., and Abecasis, G.R. (2010). METAL: fast and efficient meta-analysis
1036 of genomewide association scans. Bioinformatics *26*, 2190–2191.

1037 7. Watanabe, K., Taskesen, E., van Bochoven, A., and Posthuma, D. (2017). Functional
1038 mapping and annotation of genetic associations with FUMA. Nat Commun *8*, 1826.

1039 8. Zhu, Z., Zheng, Z., Zhang, F., Wu, Y., Trzaskowski, M., Maier, R., Robinson, M.R.,
1040 McGrath, J.J., Visscher, P.M., Wray, N.R., et al. (2018). Causal associations between risk
1041 factors and common diseases inferred from GWAS summary data. Nat Commun *9*, 224.

1042 9. Liu, M., Jiang, Y., Wedow, R., Li, Y., Brazel, D.M., Chen, F., Datta, G., Davila-
1043 Velderrain, J., McGuire, D., Tian, C., et al. (2019). Association studies of up to 1.2 million
1044 individuals yield new insights into the genetic etiology of tobacco and alcohol use. Nat Genet
1045 *51*, 237–244.

1046 10. Ferreira, M.A.R., Mathur, R., Vonk, J.M., Szwajda, A., Brumpton, B., Granell, R., Brew,
1047 B.K., Ullemar, V., Lu, Y., Jiang, Y., et al. (2019). Genetic Architectures of Childhood- and
1048 Adult-Onset Asthma Are Partly Distinct. Am J Hum Genet *104*, 665–684.

1049 11. Giambartolomei, C., Vukcevic, D., Schadt, E.E., Franke, L., Hingorani, A.D., Wallace,
1050 C., and Plagnol, V. (2014). Bayesian test for colocalisation between pairs of genetic
1051 association studies using summary statistics. PLoS Genet. *10*, e1004383.

1052 12. Zhou, W., Nielsen, J.B., Fritsche, L.G., Dey, R., Gabrielsen, M.E., Wolford, B.N.,
1053 LeFaive, J., VandeHaar, P., Gagliano, S.A., Gifford, A., et al. (2018). Efficiently controlling

1054 for case-control imbalance and sample relatedness in large-scale genetic association studies.
1055 Nat. Genet. *50*, 1335–1341.

1056 13. Bulik-Sullivan, B., Finucane, H.K., Anttila, V., Gusev, A., Day, F.R., Loh, P.-R.,
1057 ReproGen Consortium, Psychiatric Genomics Consortium, Genetic Consortium for Anorexia
1058 Nervosa of the Wellcome Trust Case Control Consortium 3, Duncan, L., et al. (2015). An
1059 atlas of genetic correlations across human diseases and traits. Nat. Genet. *47*, 1236–1241.

1060 14. Wellcome Trust Case Control Consortium, Maller, J.B., McVean, G., Byrnes, J.,
1061 Vukcevic, D., Palin, K., Su, Z., Howson, J.M.M., Auton, A., Myers, S., et al. (2012).
1062 Bayesian refinement of association signals for 14 loci in 3 common diseases. Nat. Genet. *44*,
1063 1294–1301.

1064 15. Benner, C., Havulinna, A.S., Järvelin, M.-R., Salomaa, V., Ripatti, S., and Pirinen, M.
1065 (2017). Prospects of Fine-Mapping Trait-Associated Genomic Regions by Using Summary
1066 Statistics from Genome-wide Association Studies. Am J Hum Genet *101*, 539–551.

1067 16. de Leeuw, C.A., Mooij, J.M., Heskes, T., and Posthuma, D. (2015). MAGMA:
1068 generalized gene-set analysis of GWAS data. PLoS Comput. Biol. *11*, e1004219.

1069 17. Liberzon, A., Birger, C., Thorvaldsdóttir, H., Ghandi, M., Mesirov, J.P., and Tamayo, P.
1070 (2015). The Molecular Signatures Database (MSigDB) hallmark gene set collection. Cell
1071 Syst *1*, 417–425.

1072 18. Liu, Y., and Xie, J. (2020). Cauchy Combination Test: A Powerful Test With Analytic *p* -
1073 Value Calculation Under Arbitrary Dependency Structures. Journal of the American
1074 Statistical Association *115*, 393–402.

1075 19. Liu, Y., Chen, S., Li, Z., Morrison, A.C., Boerwinkle, E., and Lin, X. (2019). ACAT: A
1076 Fast and Powerful p Value Combination Method for Rare-Variant Analysis in Sequencing
1077 Studies. Am. J. Hum. Genet. *104*, 410–421.

1078 20. Turkmen, A., and Lin, S. (2017). Are rare variants really independent? Genet. Epidemiol.
1079 *41*, 363–371.

1080 21. Talluri, R., and Shete, S. (2013). A linkage disequilibrium-based approach to selecting
1081 disease-associated rare variants. PLoS ONE *8*, e69226.

1082 22. Gusev, A., Ko, A., Shi, H., Bhatia, G., Chung, W., Penninx, B.W.J.H., Jansen, R., de
1083 Geus, E.J.C., Boomsma, D.I., Wright, F.A., et al. (2016). Integrative approaches for large-
1084 scale transcriptome-wide association studies. Nat. Genet. *48*, 245–252.

1085 23. Mancuso, N., Freund, M.K., Johnson, R., Shi, H., Kichaev, G., Gusev, A., and Pasaniuc,
1086 B. (2019). Probabilistic fine-mapping of transcriptome-wide association studies. Nat. Genet.
1087 *51*, 675–682.

1088 24. Zheng, J., Erzurumluoglu, A.M., Elsworth, B.L., Kemp, J.P., Howe, L., Haycock, P.C.,
1089 Hemani, G., Tansey, K., Laurin, C., Early Genetics and Lifecourse Epidemiology (EAGLE)
1090 Eczema Consortium, et al. (2017). LD Hub: a centralized database and web interface to
1091 perform LD score regression that maximizes the potential of summary level GWAS data for
1092 SNP heritability and genetic correlation analysis. Bioinformatics *33*, 272–279.

1093 25. O'Connor, L.J., and Price, A.L. (2018). Distinguishing genetic correlation from causation
1094 across 52 diseases and complex traits. Nat. Genet. *50*, 1728–1734.

1095 26. Reay, W.R., Kiltschewskij, D.J., Geaghan, M.P., Atkins, J.R., Carr, V.J., Green, M.J., and
1096 Cairns, M.J. (2021). Genetic estimates of correlation and causality between blood-based
1097 biomarkers and psychiatric disorders (Psychiatry and Clinical Psychology).

1098 27. Reay, W.R., El Shair, S.I., Geaghan, M.P., Riveros, C., Holliday, E.G., McEvoy, M.A.,
1099 Hancock, S., Peel, R., Scott, R.J., Attia, J.R., et al. (2021). Genetic association and causal
1100 inference converge on hyperglycaemia as a modifiable factor to improve lung function. ELife
1101 *10*, e63115.

1102 28. Hemani, G., Zheng, J., Elsworth, B., Wade, K.H., Haberland, V., Baird, D., Laurin, C.,
1103 Burgess, S., Bowden, J., Langdon, R., et al. (2018). The MR-Base platform supports
1104 systematic causal inference across the human phenome. ELife *7*, e34408.

1105 29. Willer, C.J., Schmidt, E.M., Sengupta, S., Peloso, G.M., Gustafsson, S., Kanoni, S.,
1106 Ganna, A., Chen, J., Buchkovich, M.L., Mora, S., et al. (2013). Discovery and refinement of
1107 loci associated with lipid levels. Nat Genet *45*, 1274–1283.

1108 30. Bowden, J., Davey Smith, G., Haycock, P.C., and Burgess, S. (2016). Consistent
1109 Estimation in Mendelian Randomization with Some Invalid Instruments Using a Weighted
1110 Median Estimator. Genet. Epidemiol. *40*, 304–314.

1111 31. Hartwig, F.P., Davey Smith, G., and Bowden, J. (2017). Robust inference in summary
1112 data Mendelian randomization via the zero modal pleiotropy assumption. Int J Epidemiol *46*,
1113 1985–1998.

1114 32. Bowden, J., Davey Smith, G., and Burgess, S. (2015). Mendelian randomization with
1115 invalid instruments: effect estimation and bias detection through Egger regression. Int J
1116 Epidemiol *44*, 512–525.

1117 33. Verbanck, M., Chen, C.-Y., Neale, B., and Do, R. (2018). Detection of widespread
1118 horizontal pleiotropy in causal relationships inferred from Mendelian randomization between
1119 complex traits and diseases. Nat. Genet. *50*, 693–698.

1120 34. Thompson, S.G., and Sharp, S.J. (1999). Explaining heterogeneity in meta-analysis: a
1121 comparison of methods. Stat Med *18*, 2693–2708.

1122 35. Bowden, J., Del Greco M, F., Minelli, C., Davey Smith, G., Sheehan, N., and Thompson,
1123 J. (2017). A framework for the investigation of pleiotropy in two-sample summary data
1124 Mendelian randomization. Stat Med *36*, 1783–1802.

1125 36. Reay, W.R., Shair, S.E., Geaghan, M.P., Riveros, C., Holiday, E.G., McEvoy, M.A.,
1126 Hancock, S., Peel, R., Scott, R.J., Attia, J.R., et al. (2020). Genetically informed precision
1127 drug repurposing for lung function and implications for respiratory infection (Respiratory
1128 Medicine).

1129 37. Reay, W.R., Atkins, J.R., Carr, V.J., Green, M.J., and Cairns, M.J. (2020).
1130 Pharmacological enrichment of polygenic risk for precision medicine in complex disorders.
1131 Sci Rep *10*, 879.

38. Sudlow, C., Gallacher, J., Allen, N., Beral, V., Burton, P., Danesh, J., Downey, P., Elliott, P., Green, J., Landray, M., et al. (2015). UK biobank: an open access resource for identifying the causes of a wide range of complex diseases of middle and old age. PLoS Med *12*, e1001779.

39. Bycroft, C., Freeman, C., Petkova, D., Band, G., Elliott, L.T., Sharp, K., Motyer, A., Vukcevic, D., Delaneau, O., O'Connell, J., et al. (2018). The UK Biobank resource with deep phenotyping and genomic data. Nature *562*, 203–209.

40. Choi, S.W., and O'Reilly, P.F. (2019). PRSice-2: Polygenic Risk Score software for biobank-scale data. GigaScience *8*, giz082.

41. Mentzer, A.J., Brenner, N., Allen, N., Littlejohns, T.J., Chong, A.Y., Cortes, A., Almond, R., Hill, M., Sheard, S., McVean, G., et al. (2019). Identification of host-pathogen-disease relationships using a scalable Multiplex Serology platform in UK Biobank (Infectious Diseases (except HIV/AIDS)).

42. Gu, Z., Eils, R., and Schlesner, M. (2016). Complex heatmaps reveal patterns and correlations in multidimensional genomic data. Bioinformatics *32*, 2847–2849.

43. Linden, S.K., Sutton, P., Karlsson, N.G., Korolik, V., and McGuckin, M.A. (2008). Mucins in the mucosal barrier to infection. Mucosal Immunol *1*, 183–197.

44. Chen, H.-H., Shaw, D.M., Petty, L.E., Graff, M., Bohlender, R.J., Polikowsky, H.G., Zhong, X., Kim, D., Buchanan, V.L., Preuss, M.H., et al. (2021). Host genetic effects in pneumonia. The American Journal of Human Genetics *108*, 194–201.

45. Campos, A.I., Kho, P.F., Vazquez-Prada, K.X., García-Marín, L.M., Martin, N.G., Cuéllar-Partida, G., and Rentería, M.E. (2020). Genetic susceptibility to pneumonia: A GWAS meta-analysis between UK Biobank and FinnGen (Respiratory Medicine).

46. Kim, K., Park, S., Park, S.Y., Kim, G., Park, S.M., Cho, J.-W., Kim, D.H., Park, Y.M., Koh, Y.W., Kim, H.R., et al. (2020). Single-cell transcriptome analysis reveals TOX as a promoting factor for T cell exhaustion and a predictor for anti-PD-1 responses in human cancer. Genome Med *12*, 22.

47. Sekine, T., Perez-Potti, A., Nguyen, S., Gorin, J.-B., Wu, V.H., Gostick, E., Llewellyn-Lacey, S., Hammer, Q., Falck-Jones, S., Vangeti, S., et al. (2020). TOX is expressed by exhausted and polyfunctional human effector memory $CD8^+$ T cells. Sci. Immunol. *5*, eaba7918.

48. Lin, C.-L., Liu, T.-C., Chung, C.-H., and Chien, W.-C. (2018). Risk of pneumonia in patients with insomnia: A nationwide population-based retrospective cohort study. J Infect Public Health *11*, 270–274.

49. Patel, S.R., Malhotra, A., Gao, X., Hu, F.B., Neuman, M.I., and Fawzi, W.W. (2012). A prospective study of sleep duration and pneumonia risk in women. Sleep *35*, 97–101.

50. Burgess, S., and Thompson, S.G. (2015). Multivariable Mendelian randomization: the use of pleiotropic genetic variants to estimate causal effects. Am J Epidemiol *181*, 251–260.

1170 51. Parr, J.B. (2020). Time to Reassess Tocilizumab's Role in COVID-19 Pneumonia. JAMA
1171 Intern Med.

1172 52. Folkersen, L., Fauman, E., Sabater-Lleal, M., Strawbridge, R.J., Frånberg, M., Sennblad,
1173 B., Baldassarre, D., Veglia, F., Humphries, S.E., Rauramaa, R., et al. (2017). Mapping of 79
1174 loci for 83 plasma protein biomarkers in cardiovascular disease. PLoS Genet *13*, e1006706.

1175 53. Ferreira, R.C., Freitag, D.F., Cutler, A.J., Howson, J.M.M., Rainbow, D.B., Smyth, D.J.,
1176 Kaptoge, S., Clarke, P., Boreham, C., Coulson, R.M., et al. (2013). Functional IL6R 358Ala
1177 allele impairs classical IL-6 receptor signaling and influences risk of diverse inflammatory
1178 diseases. PLoS Genet *9*, e1003444.

1179 54. Davis, W.A., Knuiman, M., Kendall, P., Grange, V., Davis, T.M.E., and Fremantle
1180 Diabetes Study (2004). Glycemic exposure is associated with reduced pulmonary function in
1181 type 2 diabetes: the Fremantle Diabetes Study. Diabetes Care *27*, 752–757.

1182 55. King, J.B., West, M.B., Cook, P.F., and Hanigan, M.H. (2009). A novel, species-specific
1183 class of uncompetitive inhibitors of gamma-glutamyl transpeptidase. J Biol Chem *284*, 9059–
1184 9065.

1185 56. Tuzova, M., Jean, J.-C., Hughey, R.P., Brown, L.A.S., Cruikshank, W.W., Hiratake, J.,
1186 and Joyce-Brady, M. (2014). Inhibiting lung lining fluid glutathione metabolism with
1187 GGsTop as a novel treatment for asthma. Front Pharmacol *5*, 179.

1188 57. Smailhodzic, D., van Asten, F., Blom, A.M., Mohlin, F.C., den Hollander, A.I., van de
1189 Ven, J.P.H., van Huet, R.A.C., Groenewoud, J.M.M., Tian, Y., Berendschot, T.T.J.M., et al.
1190 (2014). Zinc Supplementation Inhibits Complement Activation in Age-Related Macular
1191 Degeneration. PLoS ONE *9*, e112682.

1192 58. Nan, R., Tetchner, S., Rodriguez, E., Pao, P.-J., Gor, J., Lengyel, I., and Perkins, S.J.
1193 (2013). Zinc-induced self-association of complement C3b and Factor H: implications for
1194 inflammation and age-related macular degeneration. J Biol Chem *288*, 19197–19210.

1195 59. Bustamante-Marin, X.M., and Ostrowski, L.E. (2017). Cilia and Mucociliary Clearance.
1196 Cold Spring Harb Perspect Biol *9*,.

1197 60. Hewson, C.A., Haas, J.J., Bartlett, N.W., Message, S.D., Laza-Stanca, V., Kebadze, T.,
1198 Caramori, G., Zhu, J., Edbrooke, M.R., Stanciu, L.A., et al. (2010). Rhinovirus induces
1199 MUC5AC in a human infection model and in vitro via NF-κB and EGFR pathways. Eur
1200 Respir J *36*, 1425–1435.

1201 61. Barbier, D., Garcia-Verdugo, I., Pothlichet, J., Khazen, R., Descamps, D., Rousseau, K.,
1202 Thornton, D., Si-Tahar, M., Touqui, L., Chignard, M., et al. (2012). Influenza A induces the
1203 major secreted airway mucin MUC5AC in a protease-EGFR-extracellular regulated kinase-
1204 Sp1-dependent pathway. Am J Respir Cell Mol Biol *47*, 149–157.

1205 62. Singanayagam, A., Footitt, J., Kasdorf, B.T., Marczynski, M., Cross, M.T., Finney, L.J.,
1206 Trujillo Torralbo, M.-B., Calderazzo, M., Zhu, J., Aniscenko, J., et al. (2019). MUC5AC
1207 drives COPD exacerbation severity through amplification of virus-induced airway
1208 inflammation (Immunology).

1209 63. Lu, W., Liu, X., Wang, T., Liu, F., Zhu, A., Lin, Y., Luo, J., Ye, F., He, J., Zhao, J., et al.
1210 (2020). Elevated MUC1 and MUC5AC mucin protein levels in airway mucus of critical ill
1211 COVID-19 patients. J Med Virol.

1212 64. He, J., Cai, S., Feng, H., Cai, B., Lin, L., Mai, Y., Fan, Y., Zhu, A., Huang, H., Shi, J., et
1213 al. (2020). Single-cell analysis reveals bronchoalveolar epithelial dysfunction in COVID-19
1214 patients. Protein Cell *11*, 680–687.

1215 65. (2009). Essentials of Glycobiology (Cold Spring Harbor (NY): Cold Spring Harbor
1216 Laboratory Press).

1217 66. Wang, S.-S., del Solar, V., Yu, X., Antonopoulos, A., Friedman, A.E., Agarwal, K., Garg,
1218 M., Ahmed, S.M., Addya, A., Nasirikenari, M., et al. (2020). Efficient Inhibition of O-glycan
1219 biosynthesis using the hexosamine analog Ac_5 GalNTGc (Biochemistry).

1220 67. Bae, S.S., Chang, L.C., Merkin, S.S., Elashoff, D., Ishigami, J., Matsushita, K., and
1221 Charles-Schoeman, C. (2020). Major Lipids and Future Risk of Pneumonia: 20-Year
1222 Observation of the Atherosclerosis Risk in Communities (ARIC) Study Cohort. The
1223 American Journal of Medicine S0002934320306987.

1224 68. Chien, Y.-F., Chen, C.-Y., Hsu, C.-L., Chen, K.-Y., and Yu, C.-J. (2015). Decreased
1225 serum level of lipoprotein cholesterol is a poor prognostic factor for patients with severe
1226 community-acquired pneumonia that required intensive care unit admission. J Crit Care *30*,
1227 506–510.

1228 69. Antcliffe, D., Jiménez, B., Veselkov, K., Holmes, E., and Gordon, A.C. (2017).
1229 Metabolic Profiling in Patients with Pneumonia on Intensive Care. EBioMedicine *18*, 244–
1230 253.

1231 70. Nelson, M.R., Tipney, H., Painter, J.L., Shen, J., Nicoletti, P., Shen, Y., Floratos, A.,
1232 Sham, P.C., Li, M.J., Wang, J., et al. (2015). The support of human genetic evidence for
1233 approved drug indications. Nat Genet *47*, 856–860.

1234 71. Asimit, J.L., Hatzikotoulas, K., McCarthy, M., Morris, A.P., and Zeggini, E. (2016).
1235 Trans-ethnic study design approaches for fine-mapping. Eur J Hum Genet *24*, 1330–1336.

1236

1237

1238